We are IntechOpen, the world's leading publisher of Open Access books
Built by scientists, for scientists

6,900
Open access books available

186,000
International authors and editors

200M
Downloads

154
Countries delivered to

Our authors are among the

TOP 1%
most cited scientists

12.2%
Contributors from top 500 universities

CLARIVATE ANALYTICS

BOOK CITATION INDEX

INDEXED

WEB OF SCIENCE™

Selection of our books indexed in the Book Citation Index
in Web of Science™ Core Collection (BKCI)

Interested in publishing with us?
Contact book.department@intechopen.com

Numbers displayed above are based on latest data collected.
For more information visit www.intechopen.com

2 µm Laser Sources
and Their Possible Applications

Karsten Scholle, Samir Lamrini, Philipp Koopmann and Peter Fuhrberg
LISA laser products OHG
Germany

1. Introduction

The wavelength range around 2 µm which is covered by the laser systems described in this chapter is part of the so called "eye safe" wavelength region which begins at about 1.4 µm. Laser systems that operate in this region offer exceptional advantages for free space applications compared to conventional systems that operate at shorter wavelengths. This gives them a great market potential for the use in LIDAR and gas sensing systems and for direct optical communication applications. The favourable absorption in water makes such lasers also very useful for medical applications. As it can be seen in figure 1, there is a strong absorption peak near 2 µm which reduces the penetration depth of this wavelength in tissue to a few hundred µm.
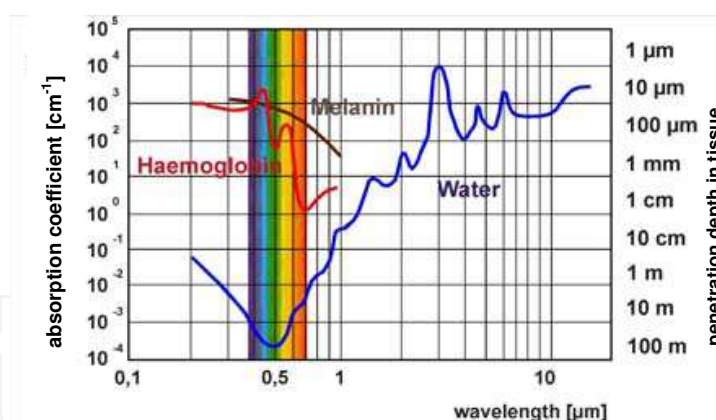

Fig. 1. Absorption and penetration depth in water and other biological tissue constituents for different wavelengths

Due to the strong absorption in water, the main constituent of biological tissue, substantial heating of small areas is achieved. This allows for very precise cutting of biological tissue. Additionally the bleeding during laser cutting is suppressed by coagulation, this makes 2 µm lasers ideal for many surgical procedures.

Furthermore 2 µm lasers are well suited to measure the health of planet earth. They can be used directly for measuring the wind velocity and for the detection of both water vapour and carbon dioxide concentration. Wind sensing is very important for weather forecasting, storm tracking, and airline safety. Water vapour and carbon dioxide detection is useful for weather and climate prediction and for the analysis of the green house effect.

2. Solid state laser systems around 2 μm

In the wavelength range around 2 μm the most interesting transitions for high power continuous wave (cw) and pulsed laser operation exist in the trivalent rare earth ions Tm^{3+} and Ho^{3+}. Using these ions laser emission was achieved in many different host crystals and glass fibres. For cw operation the thulium lasers are most interesting; however for pulsed and q-switched operation holmium lasers are more attractive due to the higher gain of the holmium doped crystals. The first experiments with Tm^{3+} and Ho^{3+} doped crystals were already carried out in the 1960s (Johnson, 1963). For both ions the relevant laser transition for the 2 μm emission ends in the upper Stark levels of the ground state. Therefore both lasers can be described as quasi three level lasers with a thermally populated ground state (Svelto, 1998; Koechner, 2006). Thulium lasers have the great advantage that the Tm^{3+} ions can be directly excited with commercially available laser diodes around 800 nm. To achieve efficient laser operation at 2.1 μm holmium can only be excited directly around 1.9 μm or by exploiting an energy transfer process from thulium or ytterbium.

2.1 Thulium lasers systems

With thulium doped crystals laser emission on many different transitions was reached so far. The laser emission around 2.0 μm is resulting from a transition that starts in the $^3F_4$ manifold and ends in a thermally populated Stark level of the $^3H_6$ ground state. The first Tm:YAG laser at 2 μm using this transition was realised in 1965 (Johnson et al., 1965). It was a flash lamp pumped laser which operated at 77 K. It took some years until the first pulsed laser operation at room temperature was realised in 1975 using Cr,Tm:YAG (Caird et al., 1975). Shortly after the development of the first laser diodes in the wavelength range around 800 nm continuous wave diode pumped laser operation at room temperature was shown (Huber et al., 1988; Becker et al., 1989). Until now thulium laser emission around 2 μm was demonstrated in many different host materials and there are some thulium based laser systems commercially available (LISA laser products OHG; IPG Photonics Corp.).

The energy level scheme of Tm^{3+} with the relevant energy transfer processes for this laser transition is shown in figure 2. The scheme of Tm:YAG is shown, as YAG is the most commonly used host material for thulium lasers. The figure also shows the Stark splitting of the ground state, which is important for the thermal population of the lower laser level of the 2 μm laser transition. In the figure one can see that the thulium ions can be excited around 800 nm from the ground state to the $^3H_4$ energy level. The upper laser level $^3F_4$ is then populated by a cross relaxation process (CR) that occurs between two thulium ions. In this non-radiative process for one ion an electron relaxes from the $^3H_4$ level to the $^3F_4$ level and for a second ion an electron is excited from the ground state to the $^3F_4$ level (French et al., 1992; Becker et al., 1989). This excitation process yields two excited ions for each absorbed pump photon. Therefore the quantum efficiency is nearly two when the cross relaxation process is highly efficient. Thus, instead of a maximum efficiency of 41 %, one can obtain an efficiency of 82 %, in theory. The efficiency of the cross relaxation process depends on the doping concentration of the thulium ions since the involved dipole-dipole interaction depends on the ion spacing. It is also possible to pump the $^3F_4$ energy level directly between 1700 nm and 1800 nm, but there are no well developed pump sources commercially available. A comparison between this direct excitation and the excitation exploiting the cross relaxation process was made by Peterson et al. (Peterson et al., 1995).

The efficiency of the laser process can be lowered by some energy transfer processes and by excited state absorption (ESA). Both possible upconversion processes that start from the upper laser level are phonon assisted. Barely any losses result from the upconversion process UC 1 which starts from the upper laser level, because this is the reverse process of the cross relaxation. More losses result from the upconversion process UC 2, because in this case the excitation of one ion is lost and another ion is excited into the $^3H_5$ level. The $^3H_5$ energy level has a very short lifetime and it is mostly depopulated by a non radiative process ($^3H_5 \rightarrow {}^3F_4$) which generates heat inside the crystal. Also excited state absorption which can start from the upper laser level $^3F_4$ or the upper level of the cross relaxation process ($^3H_4$) causes losses for the laser. The influence of these processes is usually low, due to the required phonon assistance. Only at high pump powers a slight blue fluorescence can be observed that starts from the $^1G_4$ manifold which is situated at approximately 21000 cm^{-1}.
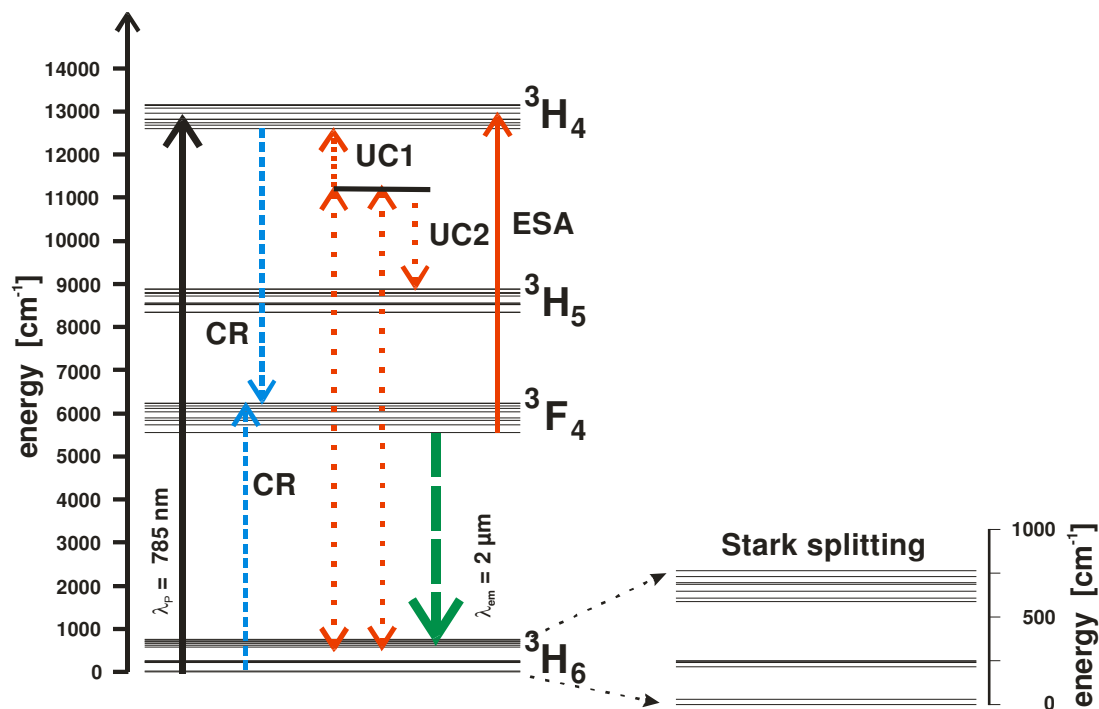

Fig. 2. Tm:YAG energy scheme with the relevant transitions for the 2 µm laser emission and the Stark splitting of the ground state

Thulium lasers have been realised in a wide variety of host crystals and fibre materials, in table 1 important parameters for the 2 µm laser transition are listed for a selection of crystals used for high power lasers. Further information about different thulium doped crystals can be found in the literature (Kaminskii, 1996; Sorokina & Vodopyanov, 2003). The absorption cross section σ_{abs} for the strongest absorption peak of the transition from the ground state to the $^3H_4$ manifold is given. The typical emission wavelength for the free running laser λ_{em} and the emission cross section for this transition σ_{em} are shown. For a comparison of the suitability of the different host materials for the laser operation the thermal conductivity λ_{th} and the lifetime of the upper laser level τ are listed.

The thermal conductivity of the host material is very important for the laser operation. The generated heat in the laser crystal has to be dissipated and removed efficiently to achieve high output powers. As it can be seen in table 1 the thermal conductivity of YLF is very low and it is rather high for Sc_2O_3, for YAG it is in between. The thermal conductivities are

measured with un-doped crystals, but normally the thermal conductivity is reduced significantly with higher thulium doping concentrations (Gaumé et al., 2003). The heat removal from the laser material can be increased by using special geometries like thin disks or slabs instead of the standard rod geometry.

The lifetime of the upper laser level τ also depends on the thulium doping concentration of the crystal. In table 1 the lifetimes are given for very low doping concentrations, with higher thulium doping concentrations the lifetimes are often strongly reduced (Scholle et al., 2004). The main reason for this effect is the increased energy migration between the Tm^{3+} ions which supports the energy transfer to crystal impurities. The longest lifetimes of 15.6 ms of the upper laser level were measured for Tm:YLF crystals, which are about 1.5 times longer than in Tm:YAG and up to four times longer then for $Tm:Lu_2O_3$ and $Tm:Sc_2O_3$ crystals. Longer lifetimes allow larger energy storage in the upper laser level which is essentially important for q-switching operation.

laser host material	σ_{abs} $(10^{-21}\, cm^2)$	λ_{em} (nm)	σ_{em} $(10^{-21}\, cm^2)$	λ_{th} $(W\, m^{-1}\, K^{-1})$	τ (ms)	reference
YAG	7.5	2013	1.8	13	10	Heine, 1995
YLF	σ pol 3.6 π pol 8.0	1910 1880	2.35 3.7	6	15.6	Payne et al., 1992 Walsh et al., 1998
Lu_2O_3	3.8	2070 1945	2.3 8.5	13	3.8	Koopmann et al., 2009a
Sc_2O_3	5.0	1994	8.4	17	4.0	Fornasiero et al., 1999
Y_2O_3	5.0	2050 1932	2.1 8.1	14		Ermeneux et al., 1999
LuAG	5.7	2023	1.66	13	10.9	Scholle et al., 2004
$YAlO_3$		1936	5.0	11	4.8	Payne et al., 1992
silica fibre	4.5	1860	3.9		6.6	Agger & Povlsen, 2006
germanate f.	6	1840	4.1		5.3	Turri et al.,2008

Table 1. Properties of widely used thulium doped laser crystals for high power applications. Absorption cross section σ_{abs}; free running laser emission wavelength λ_{em}; emission cross section σ_{em}; thermal conductivity λ_{th}; lifetime of the upper laser level τ.

As mentioned, thulium 2 µm lasers can be pumped around 800 nm, exploiting the cross relaxation process to populate the upper laser level. Tm:YAG has one of the highest absorption cross sections in this wavelength region, but the main absorption peak is located at 785 nm. Figure 3 shows the absorption spectra of Tm:YAG, $Tm:Lu_2O_3$ and Tm:YLF. Tm:YLF has a natural birefringence, therefore the spectra for π and σ polarisation are shown.

A challange for most of the thulium doped crystals is that the available diodes around 800 nm where mainly developed for Nd:YAG pumping at 808 nm. So the available diodes in the range from 785 – 795 nm are more expensive and possess lower brightness and output powers compared to those operating close to 808 nm. Therefore most of the Tm doped crystals can not be pumped at the strongest absorption peak, only thulium doped sesquioxides like Lu_2O_3 and some vanadates have strong absorption lines near 808 nm. Due to the weak absorption larger crystals or multi pump pass set-ups have to be used to achieve sufficient pump light absorption.
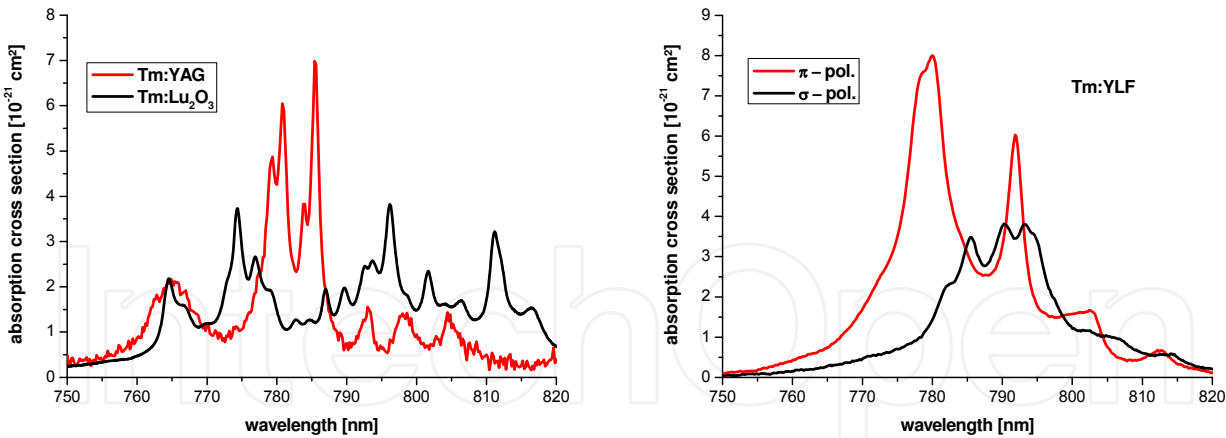
Fig. 3. Absorption cross sections of the $^3H_6 \rightarrow \,^3H_4$ transition for Tm:YAG, Tm:Lu$_2$O$_3$, (Koopmann et al. 2009b) and Tm:YLF.

As can be seen in table 1, the different host materials provide the possibility to access many wavelengths in the range between 1840 nm and 2100 nm with thulium lasers. In the table the emission cross sections are shown for the typical free running laser transition, but thulium has a very broad and strongly structured emission spectrum in most crystals. As an example the emission spectra for Tm:YAG, Tm:Lu$_2$O$_3$ and Tm:YLF are shown in figure 4. One can see that the emission cross sections of Tm:YAG are much lower than for Tm:YLF and most other crystals. Low emission cross sections lead to low gain, therefore in YAG a co-doping of thulium and holmium was often used in the past since holmium has six times larger emission cross sections in YAG.
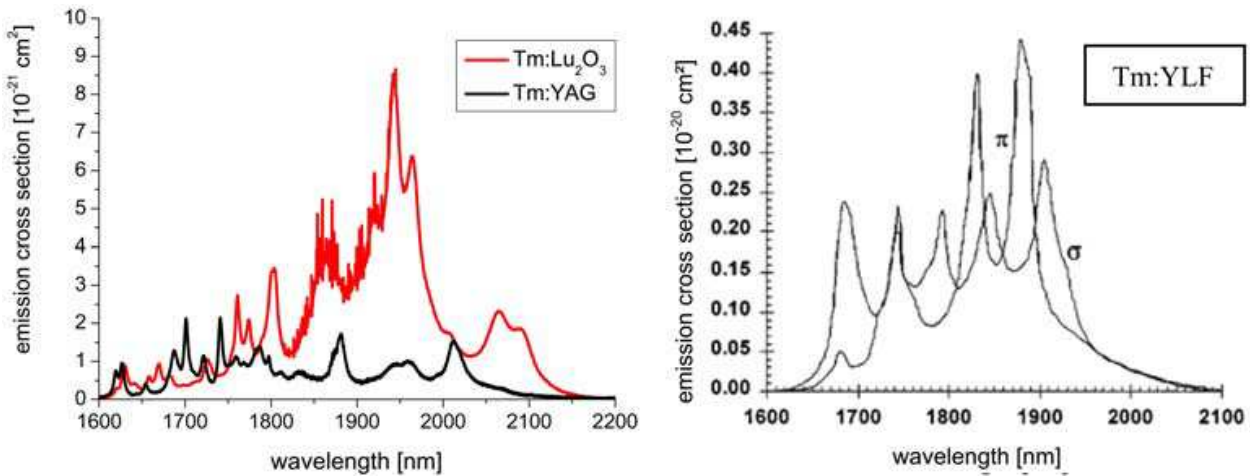

Fig. 4. Left side: Emission cross sections of Tm:YAG and Tm:Lu$_2$O$_3$ for the transitions from the $^3F_4$ manifold to the ground state (Koopmann et al., 2009b). Right side: Emission cross sections for π and σ polarisation of Tm:YLF (Budni et al., 2000).

The broad emission spectra of thulium doped crystals enable very large wavelength tuning ranges for thulium laser systems. This is very useful for a couple of laser applications. Additionally a broad gain spectrum allows the generation of extremely short laser pulses in mode-locked laser operation. Wavelength tuning is achieved by integration of wavelength selective elements into the laser resonator. Mostly prisms, diffraction gratings or birefringent filters under Brewster angle are used for wavelength tuning (Svelto, 1998). Tuning ranges of over 200 nm were achieved in different thulium doped crystals so far, for

instance the tuning curves for Tm:LuAG and Tm:Lu$_2$O$_3$ are shown in figure 5. Tm:LuAG can only be sufficiently operated from 2010 nm to 2040 nm. With Tm:Lu$_2$O$_3$ efficient laser operation is possible from 1900 nm to 2110 nm. Especially the tuning range up to 2.1 µm with high output powers makes Tm:Lu$_2$O$_3$ attractive, since this laser can be an alternative to Ho:YAG lasers that emit around this wavelength.
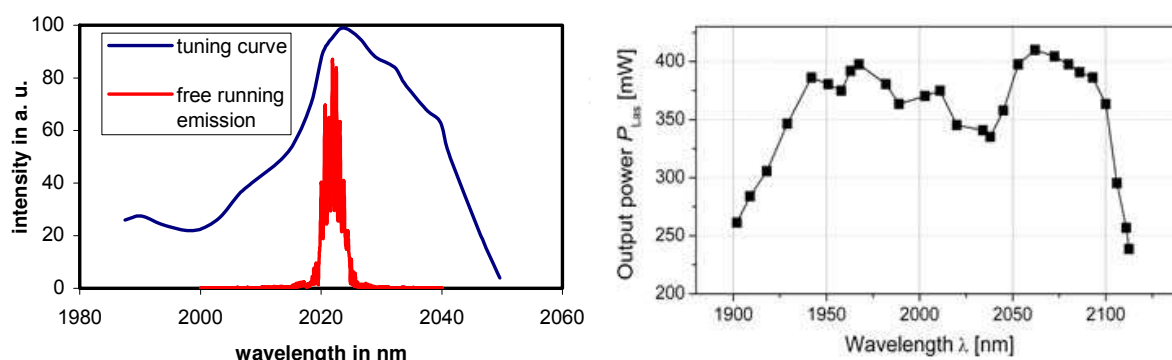
Fig. 5. Tuning curves of Tm:LuAG (Scholle et al., 2004) and Tm:Lu$_2$O$_3$ (Koopmann et al., 2009a)

Some of the important parameters of thulium doped crystals for laser operation around 2 µm have been discussed, but there are still some more aspects, which are important for the realisation of a high power thulium laser. A very important point is the crystal quality. To achieve high output powers, high quality crystals with very few impurities and defects are necessary. Additionally the achievable crystal size is important. In big crystals the generated heat can be distributed over a larger area. For rod or slab lasers much larger crystals than for thin disc lasers are required. The best qualities and largest crystal sizes are achieved today with Tm:YAG and Tm:YLF, but these crystals are not the best choice regarding thermal conductivity or emission cross section. Therefore in the future other host crystals like Lu$_2$O$_3$ or Sc$_2$O$_3$ can become important when larger high quality crystals become available.

Although thulium lasers have been realised in many different host crystals, high power lasers with output powers of some tens of watts or even more have been demonstrated only with YAG and YLF as laser host materials so far. In table 2 a short overview of some recently published thulium crystal and fibre laser systems is shown. The first high power thulium lasers were realised with solid state systems, nowadays the fibre laser system deliver the highest output powers.

The first cw diode pumped thulium 2 µm laser with output powers > 100 W was demonstrated in 1997 (Honea et al., 1997). To achieve these high output powers, Tm:YAG rods with undoped YAG end caps were used. The end caps were diffusion bonded to the doped rod to optimise the cooling of the rods and to reduce the thermal stress on the end surfaces. The laser rod was end-pumped by a diode bar operating at 805 nm using a fused silica lens duct to couple the pump light into the rod of 3 mm in diameter. With such a set-up and a 2 % thulium doped rod in a short plane-concave laser cavity up to 115 W of output power at room temperature were achieved. The laser showed a high slope efficiency of about 52 %, however the beam quality was poor at high powers (M^2 = 23). Nowadays Tm:YAG lasers emitting at 2.0 µm are commercially available. For instance LISA laser products OHG offers the RevoLix 120 Watt laser system, which is a medically approved Tm:YAG laser system. This system is used for non-invasive surgery, where the laser light

needs to be delivered by a fibre. The system can deliver up to 120 W output power through different application fibres with very small core diameters.

The highest output power achieved so far with Tm:YLF rods is 55 W (Schellhorn, 2008). This high power was achieved using two 3.5 % doped Tm:YLF rods in one folded laser cavity that were pumped with four laser diodes. Each rod was pumped from both ends by a diode emitting at 792 nm. With this set-up a slope efficiency of 49 % and a beam quality of $M^2 < 3$ was observed. With a single rod the maximum output power was limited to 30 W. Due to the low thermal conductivity and the low fracture limit of Tm:YLF the rod geometry is not very well suited for high power Tm:YLF lasers. With a slab geometry further power scaling is possible, which is due to the better thermal management (So et al. 2006). The highest output power of a Tm:YLF slab reported so far is 148 W (Schellhorn et al., 2009). This was achieved with a 2 % doped Tm:YLF slab double-end-pumped by two laser diode stacks emitting at 790 nm. With an optical to optical conversion efficiency of 26.7 % 148 W of cw output power at 1912 nm were achieved at room temperature.

laser host material	λ_p (nm)	λ_{em} (nm)	cw output power (W)	slope eff. (%)	reference
YAG	805	2013	115	52	Honea et al., 1997
YAG	800	2013	120		LISA laser products OHG *
YLF	792	1910	55	49	Schellhorn, 2008
YLF	790	1912	148	32.6	Schellhorn et al., 2009
Lu_2O_3	796	2070	1.5	61	Koopmann et al., 2009a
germanate f.	800	1900	64	68	Wu et al., 2007
silica fibre	793	2050	110	55	Frith et al., 2007
silica fibre	1567	1940	415	60	Meleshkevich et al., 2007
silica fibre	790	2040	885	49.2	Moulton et al., 2009

Table 2. Brief overview of recently published continuous wave thulium solid state and fibre laser results (λ_p = pump wavelength; λ_{em} = emission wavelength). * RevoLix 120 Watt commercial system from LISA laser products OHG

Nowadays nearly the same maximum output powers can be reached with Tm:YAG and Tm:YLF lasers. The slope efficiencies of the Tm:YAG systems are higher than for the Tm:YLF ones, but the beam quality of the Tm:YLF systems is better due to the weaker thermal lenses which occur in YLF. Further power scaling of the output power from both systems should be possible especially with the slab geometry. So far the maximum reported output powers were limited by the available pump powers, not by fracture of the laser crystals. Great potential for power scaling is also exhibited by $Tm:Lu_2O_3$. The properties of the crystal and the recently reported results with record high slope efficiencies indicate the large potential of this crystal.

In recent years a lot of research has been performed on the improvements of fibre lasers and great advances were made in the power scaling. Since the late 1980s for many years single-mode diode pumped fibre lasers that emitted a few tens of milliwatts were used because of their large gain and the feasibility of single-mode continuous wave lasing. The most well-known application of these fibre lasers is in the telecom market around 1550 nm where erbium-doped fibre lasers and amplifiers are used. The modern high-power fibre lasers are built mostly with double-clad fibres that have a small inner core that is doped with the laser active ions and is surrounded by a much larger cladding. These fibres can be pumped by

high-power multimode diodes or even diode bars or stacks. The pump light is guided in the cladding by total internal reflection between the cladding and the coating and it is only absorbed when it passes through the doped core of the fibre. This fibre design concept allows the efficient conversion of multimode laser diode radiation into fibre laser radiation with very high brightness.

Today, the highest output powers of fibre lasers (some kW) have been demonstrated with ytterbium doped silica fibres that operate in the wavelength region centred around 1080 nm. Lasers in this wavelength range are not "eye safe" which is a problem for a lot of laser applications. But nowadays also thulium doped fibres almost reach the kW output power level. A selection of the latest publications reporting on high power thulium fibre lasers around 2.0 μm is shown in table 2. The fibre geometry has the great advantage that the heat that is generated during the laser process is dissipated over a large area if a long absorption distance is used. The absorption length of a fibre system can be adjusted not only by the doping concentration and the pump wavelength, also the core to cladding ratio can be used.

In 2007 Frith et al. reported on a highly efficient thulium fibre laser with up to 110 W of cw output power. They used newly designed large mode area fibres which yield a low numerical aperture (NA) of the doped core (NA = 0.06). This enables the usage of large core diameters by still retaining single transversal mode laser operation. Therefore Frith et al. could build up a laser using a fibre with a core diameter of 20 μm, a cladding diameter of 400 μm, and a fibre Bragg grating as a highly reflective mirror. With this concept and pumping of one fibre end through the fibre Bragg grating 110 W of narrow line width (full width at half maximum (FWHM): 3 nm) output power were achieved with a slope efficiency of 55 %. In the same year Wu et al. reported on the high power operation of a thulium doped germanate fibre (Wu et al., 2007). They achieved 64 W of output power in a one-end pumped configuration with an only 20 cm long piece of fibre. With respect to the launched 800 nm pump power an extremely high slope efficiency of 68 % was measured. In a dual-end pumped configuration the maximum output power could be increased to 104 W, but the slope efficiency was reduced to 52.5 %. Also in 2007 a 415 W thulium fibre laser that was inband pumped at 1567 nm was presented (Meleshkevich et al., 2007). A double clad single mode thulium fibre was used, which was end pumped by an assembly of 18 cw erbium fibre lasers. By the usage of fibre Bragg gratings an all-fibre set-up was realised which yielded an output beam with $M^2 < 1.1$ and a slope efficiency of 60 %. Using a thulium doped fibre with a core diameter of 35 μm (numerical aperture 0.2) and a cladding diameter of 625 μm Moulton et al. achieved a cw output power of up to 885 W at room temperature (Moulton et al., 2009). This is the highest output power achieved with a single Tm-doped fibre so far. The laser showed multi mode emission with a slope efficiency of about 49.2 %. To achieve this high output power a 7 m long piece of fibre was used that was pumped from both ends with fibre coupled laser diode sources emitting at 793 nm. So actually the highest thulium fibre laser output powers were achieved with diode pumping around 800 nm, but also the approach with resonant pumping around 1570 nm has the potential to reach such high powers. The overall efficiency of the 800 nm pumped systems is better than for the resonant pumping due to the limited efficiency of the Yb,Er:fibre lasers used. An all fibre system should be possible with both concepts, although so far this was only presented for the resonant pumping at 1570 nm. Actually there are two companies that are offering thulium fibre lasers commercially. One offers systems that are pumped around 800 nm (Nufern) and the other is using the resonant pumping concept (IPG Photonics Corp.).

Actually the highest thulium laser output powers are achieved with fibre lasers, but also crystal lasers can reach more than 100 W of output power. The fibre lasers also yield a better beam quality than the crystal lasers, which is an enormous advantage for some applications. Both systems show approximately the same slope efficiencies, nevertheless for high output powers the optical to optical efficiency of the fibre lasers is higher. For applications with output powers in the range of 100 W to 200 W crystal lasers are still a good alternative to fibre lasers, especially since these systems are well developed and commercially available.

2.2 Holmium laser systems

Until recently there were no laser diodes available in the wavelength ranges which allow direct pumping of Ho^{3+} ions. Therefore the first holmium lasers were realised in co-doped systems. Usually thulium co-doping is used, because one can exploit the cross relaxation process of the thulium ions for the excitation of the upper laser level in holmium. There are two energy transfer processes which lead to the population of the upper laser level ($^5I_7$) of the holmium ions. The first transfer is the fast spatial energy migration among the Tm^{3+} ions and the second one is the energy transfer from the thulium $^3F_4$ to the holmium $^5I_7$ level. The net energy transfer can be determined as

$$f_{Ho} = \frac{N_{Ho} \cdot \sum_i g_i \cdot e^{-\frac{E_i}{k \cdot T}}}{N_{Ho} \cdot \sum_i g_i \cdot e^{-\frac{E_i}{k \cdot T}} + N_{Tm} \cdot \sum_j g_j \cdot e^{-\frac{E_j}{k \cdot T}}}$$

where f_{Ho} is the net transfer efficiency, N_{Tm} is the concentration of Tm^{3+} ions, the sums over i and j are sums over the Ho^{3+} $^5I_7$ and Tm^{3+} $^3H_4$ crystal field splittings, respectively, E_i and E_j are the energy levels of these splittings, g_i and g_j are their degeneracies, k is the Boltzmann constant, and T is the temperature (Fan et al., 1988). In YAG as host crystal, about 50 % of the excitation energy is transferred to the holmium ions at room temperature when using a thulium co-doping. The rest of the energy is stored in the excited thulium ions (Storm, 1988). YAG is the most common host crystal for Ho^{3+} because of its high values of specific heat, heat conductivity and optical quality (Rothacher et al., 1998). The energy scheme of Ho:YAG with the relevant transitions for the 2.1 µm laser emission and the Stark splitting of the ground state are shown in figure 6. The 2.1 µm emission emerges from a transition which starts in the upper laser level $^5I_7$ and terminates in the thermally populated sublevels of the $^5I_8$ ground state manifold. Both involved energy levels show a strong Stark splitting, the higher level consists of 14 sublevels from 5228 cm⁻¹ to 5455 cm⁻¹ and the ground state splits up into 11 sublevels from 0 cm⁻¹ to 535 cm⁻¹ (Kaminskii, 1996).

The thermal population of the lower laser level at room temperature for the free running Ho:YAG laser is about 2 %, which is nearly the same as for the Tm:YAG laser. But the upper laser level of the holmium laser is also thermally populated and this population is much lower than for thulium lasers. At room temperature in YAG only 10 % of the holmium ions, which are excited to the $^5I_7$ manifold, populate the Stark level which is the upper laser level. For thulium this number is about 46 %. Therefore the temperature dependence of holmium lasers is stronger than the one of thulium lasers. The upconversion process, in which one holmium ion gets excited into the $^5I_5$ or the $^5I_6$ manifold, is a non resonant process (see figure 6). It is a phonon assisted process, for which two closely spaced holmium ions that are

excited into the $^5I_7$ manifold are necessary. Therefore this process becomes important when the population density of the $^5I_7$ energy level is high. Thus the upconversion process is most important for the q-switched operation, when the energy storage in the upper laser level is high.
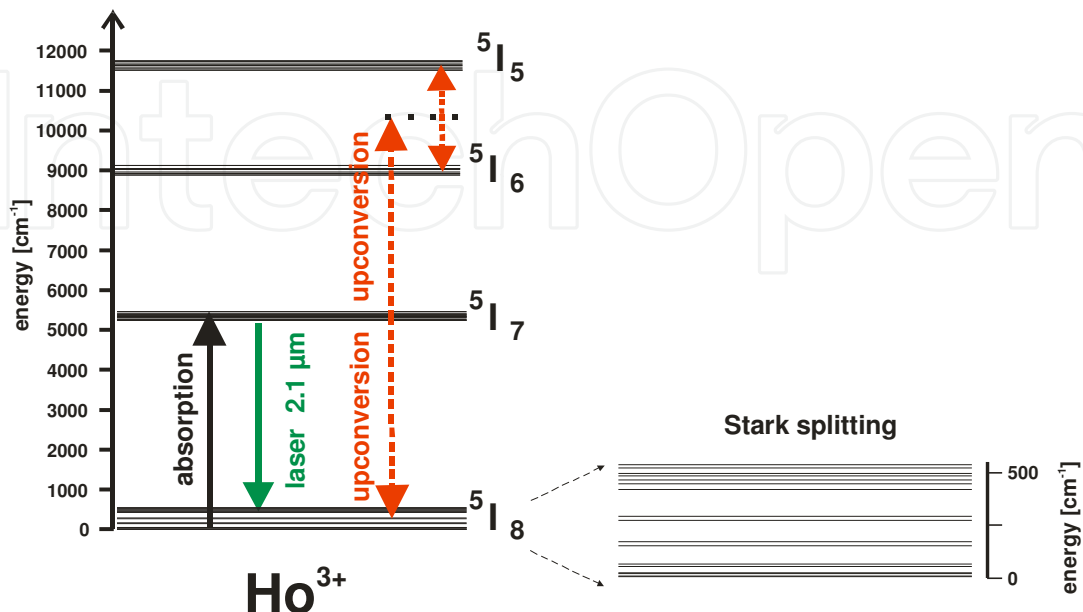

Fig. 6. Ho:YAG energy scheme with the relevant transitions for 2.1 μm laser operation

The first holmium laser on the 2.1 μm transition used a thulium co-doping and YAG as a host material. It was a flash lamp pumped pulsed laser that was built up in 1965 (Johnson et al., 1965; Johnson et al., 1966). This laser needed to be cooled with liquid nitrogen. Room temperature, lamp pumped, pulsed operation of Ho:YAG and Ho:YLF lasers was demonstrated in 1970 and 1971, respectively (Remski et al., 1970; Chicklis et al., 1971). The investigated crystals were sensitised with Er^{3+} and Tm^{3+}, leading to an optimised absorption of the pump light. The first room temperature cw laser operation of a holmium laser with thulium co-doping was demonstrated in 1985, using a krypton laser as pump source (Duczynski et al., 1986). Shortly after the development of diode lasers around 800 nm many innovative approaches of pumping thulium co-doped holmium lasers were successfully realised. The first cw holmium lasers utilising diode pumping were demonstrated in 1986 for YAG as host material and for YLF in 1987 (Fan et al., 1987; Kintz et al., 1987). Intra-cavity pumping of Ho:YAG was demonstrated for the first time in 1992 (Stoneman et al., 1992). The Ho:YAG crystal was embedded in a Tm:YAG laser cavity and acted as output coupler.
The following section focuses on the latest results of different methods for in-band pumping (direct pumping into the upper laser level $^5I_7$) of Ho:YAG crystals, which is the most promising approach to reach the highest output powers. In-band pumping of most holmium crystals is possible in the wavelength range around 1.9 μm. The latest results of continuous wave and q-switched holmium laser operation will be shown and reviewed. The co-doping of thulium and holmium in crystals and fibres has significant drawbacks. The probability of the upconversion process that populates the $^5I_5$ and the $^5I_6$ level is increased by the co-doping and the thermal load in the crystal is higher, even when the cross relaxation process of the thulium ions is exploited very well. Due to the fact that the emission wavelength of 2.1 μm addresses a wide variety of applications that require short laser pulses with high

pulse energies or high continuous wave powers, many high power holmium laser systems were realised in recent years. Most of these laser systems use thulium crystal or fibre lasers for pumping the holmium ions. An overview of some of the latest published results is shown in table 3.

laser material	pump source	λ_p (μm)	cw power (W)	pulse energy (mJ)	λ_{em} (nm)	slope. eff. (%)	reference
Ho:YAG	Tm:YLF	1.95	1.6		2090	21	Schellhorn et al., 2003
Ho:YAG	Tm:YLF	1.9		50	2090		Budni et al., 2003
Ho:YAG	Tm fibre	1.905	6.4		2097	80	Shen et al., 2004
Ho:YLF	Tm fibre	1.94	43	40	2050	42	Dergachev et al., 2005
Ho:YAG	Tm fibre	1.908	10	15	2100	52	Moskalev et al., 2006
Ho:YAG	Tm:YLF	1.908	9.4		2090	40	Schellhorn, 2006
Ho:YAG	Tm:YLF	1.91	14		2100	16	So et al., 2006b
Ho:YAG	diode	1.91	40	3.5	2120	57	Scholle & Fuhrberg 2008
Ho:YLF	Tm fibre	1.94	12.4	10.9	2065	47	Bollig et al., 2009
Ho:YAG	Tm fibre	1.908	18.7		2090	80	Mu et al., 2009

Table 3. Overview of some recently published cw and pulsed holmium laser results in the literature (λ_p = pump wavelength; λ_{em} = emission wavelength)

Thulium fibre lasers are an excellent pump source for holmium lasers. They offer a nearly diffraction limited beam quality and a very narrow emission bandwidth. The wavelength of the fibre lasers can be tuned to the maximum absorption of the holmium ions by using fibre Bragg gratings. Due to these benefits the highest slope efficiencies for in-band pumped holmium lasers were achieved with thulium fibre lasers as pump sources. Up to 80 % of slope efficiency for cw laser operation were demonstrated by Mu et al. and Shen et al. with Ho:YAG lasers. In 2004 Shen et. al. reported on a room temperature Ho:YAG laser pumped by a cladding-pumped Tm:silica-fibre laser (Shen et al., 2004). The emission wavelength of the Tm:silica-fibre laser was tuned with an external grating to the absorption maximum of Ho:YAG. With the available 9.6 W of pump power, 6.4 W of unpolarized output power of the Ho:YAG system were reached in a short plane-concave resonator. The optical to optical conversion efficiency of the system was 67 %. Mu et. al. used an adhesive free bonded YAG/Ho:YAG/YAG laser composite crystal in a water cooled heat sink (Mu et al., 2009). The front facet of the composite crystal acted as a plane highly reflective mirror for the holmium laser and the back side had a high reflectivity coating for the pump wavelength to achieve a multi pass of the pump light. Thus the resonator was built with the front facet of the crystal and a concave output coupler. The pump source, an unpolarized thulium doped fibre laser (FWHM 0.7 nm), was tuned to the strongest absorption line of Ho:YAG at 1907.65 nm. The maximum output power of this system was 18.7 W at 24.3 W of pump power, which results in an optical to optical conversion efficiency of 77.6 %, which is the highest efficiency reported so far.

In 2006, Moskalev et. al. demonstrated a q-switched Ho:YAG laser pumped by a commercially available thulium fibre laser (Moskalev et al., 2006). They used a 50 mm long Ho:YAG rod with a doping concentration of 0.5 % that was conductively cooled. With a plane concave folded cavity a maximum output power of 10 W in cw operation were demonstrated with a corresponding slope efficiency of 52 %. With an acousto-optic

modulator inside the resonator, q-switched laser operation with a maximum output power of 15 mJ at 100 Hz repetition rate was shown.

The highest cw output powers and pulse energies of a holmium laser achieved with thulium fibre laser pumping were reached with YLF as host material for the holmium ions. Dergachev et al. reached 43 W of cw output power and 40 mJ of q-switched pulse energy with a Ho:YLF laser that was pumped at 1940 nm with a commercially available 100 W thulium fibre laser (Dergachev et al., 2005). These high powers were achieved using two holmium crystals in one cavity. The crystals were pumped by one fibre laser using a polarisation beam splitter to spread the pump power. The 40 mJ of pulse energy were reached for repetition rates below 400 Hz, at 1 kHz 28 mJ of pulse energy were reached. Using a single Ho:YLF crystal Bollig et al. reached a slope efficiency of 47 % and 10.9 mJ of pulse energy at 1 kHz repetition rate (Bollig et al., 2009). With an additional Ho:YLF amplifier that was pumped by the pump light transmitted from the first holmium crystal, up to 23.7 mJ of pulse energy at 1 kHz repetition rate were reached. This amplifier system had a slope efficiency of 47 % and yielded a beam quality of $M^2 < 1.1$.

Another attractive pump source for holmium lasers are Tm:YLF lasers. Tm:YLF lasers are highly efficient and offer high pump powers with good beam quality. These laser systems can also be tuned to the maximum absorption peaks of holmium in the wavelength range between 1.9 µm and 2.0 µm. In 2003, Budni et al. demonstrated a high pulse energy q-switched Ho:YAG laser with 50 mJ of output energy and an M^2 of about 1.2, that was pumped by a Tm:YLF laser (Budni et al., 2003). They used a folded plane concave cavity, where the pump light was coupled into the holmium crystal trough a thin-film polariser that also acted as a folding mirror. Using output couplings of up to 70 % damage free q-switched operation with pulse lengths of 14 ns and peak powers of up to 3.6 MW were achieved. A Ho:YAG thin-disk laser with an output power of up to 9.4 W was realised by M. Schellhorn using two polarisation coupled Tm:YLF lasers as pump sources (Schellhorn, 2006). With a 0.4 mm thick, 2 % doped Ho:YAG crystal an optical to optical efficiency of 36 % was reached using 24 passes of the pump light through the Ho:YAG crystal.

Using Tm:YLF lasers as pump sources also intra-cavity pump schemes are possible, where the holmium crystal is placed inside the thulium laser resonator. In this case the holmium laser acts as an output coupler for the thulium laser. A schematic set-up for an intra-cavity side pumped holmium laser is shown in figure 7.
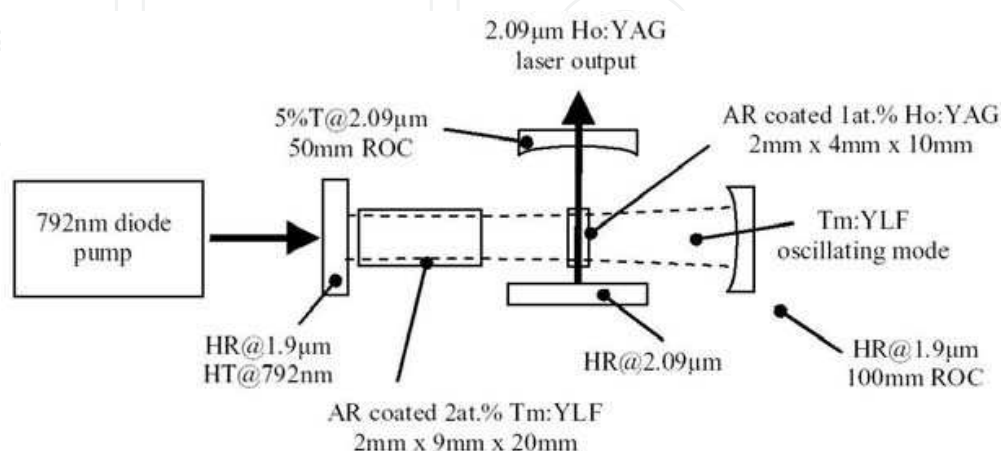

Fig. 7. Schematic diagram of a Ho:YAG intra-cavity pumped laser (So et al., 2006)

Using intra-cavity pumping a low holmium doping concentration can be used, since the pump light intensity is very high inside the laser resonator. In 2003 a compact Ho:YAG laser intra-cavity pumped by a diode-pumped Tm:YLF laser was realised (Schellhorn et al., 2003). At room temperature a maximum average holmium laser output of 1.6 W with a slope efficiency of 21 % with respect to the incident diode pump power was achieved. In 2006 So et al. demonstrated an intra-cavity side-pumped Ho:YAG laser system (So et al., 2006b). A high-power Tm:YLF slab laser (9 x 1.5 x 20 mm³) with an optimised thulium doping concentration of 2 at. % pumped by a laser diode stack at 792 nm served as the pump source. The maximum output power of the slab laser itself at a wavelength of 1.91 µm was 68 W. The corresponding slope efficiency was 44 %. The intra-cavity side-pumped Ho:YAG slab (4 x 10 x 2 mm³) had a doping concentration of 1 at. %. With the Ho:YAG slab 14 W of output power at 2.1 µm with a slope efficiency of 16 % were achieved with this set-up, which is shown in figure 7.

In all the laser systems described above the holmium lasers were pumped by thulium lasers, whose emission wavelengths were tuned to the most efficient absorption peaks of the holmium ions. These thulium laser systems are pumped with commercially available laser diodes around 800 nm. Exploiting the cross relaxation process of the thulium ions these systems reach optical to optical conversion efficiencies between 40 % and 60 %. This pumping concept yields a quite complex overall set-up and it limits the overall efficiency of the laser systems. Taking into account an electrical to optical efficiency of 50 % for the laser diodes around 800 nm the maximum overall system efficiency with these pump systems for the realised holmium lasers is about 15 %. Direct in-band pumping with laser diodes around 1.9 µm is therefore an attractive alternative to develop simple and compact holmium laser systems with high overall efficiencies.

The first directly diode in-band pumped holmium laser was realised in 1995 (Nabors et al., 1995). With six 1.9 µm laser diodes using angle multiplexing and polarisation beam combining nearly 0.7 W of output power were reached. With respect to the absorbed pump power a slope efficiency of 35 % was achieved. This demonstrated that efficient in-band pumping of Ho:YAG lasers by laser diodes at 1.9 µm is generally possible, although the emission bandwidth and the beam quality of laser diodes is inferior to thulium laser systems. Nabors et al. used a mix of GaInAsSb and InGaAsP diode lasers, each with about 0.7 W of output power, which were available in 1995. In recent years diode lasers based on GaSb material systems (AlGaIn)(AsSb) were significantly improved. They cover the wavelength range from 1.85 µm to 2.35 µm. In section 3 these diodes will be described in detail. The improvements of these high power diodes make them very interesting for the excitation of holmium lasers. The newly developed GaSb-based diode bars and stacks provide enough pump power to realise high power holmium laser systems.

Using a GaSb-based laser diode stack which consists of ten bars with an output power up to 158 W Scholle et al. presented the first high power Ho:YAG laser that was in-band pumped by such diodes in 2008 (Scholle et al., 2008). A continuous wave output power of 40 W with a slope efficiency of 57 % was demonstrated. Also q-switched operation with an acousto optic modulator (AOM) inside the laser cavity was investigated. A maximum q-switched output power of 3.5 mJ - limited by damage of the optical components - at a repetition rate of 1 kHz with 33 % output coupling was reached. The pulse durations were around 150 ns.

Using a diode stack as pump source yields some challenges for the laser set-up. In figure 8 one can see that the absorption peaks for the excitation from the ground state to the upper

laser level in Ho:YAG (left side) and Ho:YLF (right side) are narrow. The maximum absorption in Ho:YAG can be found around 1910 nm ($\sigma_{abs} = 9 \times 10^{-21}$ cm²) and the corresponding FWHM is only 7 nm. For Ho:YLF the maximum absorption depends on the polarisation, for π polarisation the maximum is at 1940 nm ($\sigma_{abs} = 10 \times 10^{-21}$ cm²) and for σ polarisation it is at 1945 nm and significantly lower ($\sigma_{abs} = 6 \times 10^{-21}$ cm²).

Fig. 8. Absorption cross sections of the $^5I_8 \rightarrow {}^5I_7$ transition for Ho:YAG and Ho:YLF (Walsh et al., 1998)

As shown in figure 14 the FWHM of the emission spectrum of a multi-bar stack is about 25 nm for high output powers, so the effective absorption coefficient in Ho:YAG for the diode stack is approximately 0.35×10^{-20} cm², when the centre wavelength of the emission is at 1910 nm. Taking this into account the absorption length of a 0.5 % doped Ho:YAG crystal is about 40 mm and for a 1 % doped crystal it is 20 mm, respectively. Another problem for pumping with diode stacks is the absorption minimum around 1895 nm, since the emission of the stack shifts over this absorption minimum when the power of the stack is continuously increased (see figure 13). When using a double pass pump scheme a significant part of the pump light can be coupled back into the diode stack, when the diode emits at this absorption minimum. This can lead to the destruction of the diode. The poor beam quality of the diode stack makes it necessary to use special optics for the collimation of the light and also for focussing into the laser rod. In our experiments the pump light of the used GaSb stack was only fast axis collimated. The slow axis divergence was compensated by a cylindrical lens inside the anti-reflective coated multi lenses focussing optic. With this optic pumping of laser rods with a diameter of 3 mm is possible. Inside the Ho:YAG rod the pump light is guide by total reflection on the polished surface of the rod.

Figure 9 shows the set-up used for the holmium laser experiments. The Ho:YAG rod and the multi-bar laser diode stack were water cooled to 15 °C with a common cooling circuit. All Ho:YAG rods used were anti reflective (AR) coated for the pump and the laser wavelength on both sides. The plane-plane resonator used for the q-switching experiments had a length of about 150 mm, for the cw experiments a shorter resonator with 80 mm in length was used. The first resonator mirror has high reflective (HR) coating for 2.1 µm and an AR coating for the pump light at 1.9 µm. After the Ho:YAG rod a pump light reflector was integrated to achieve a double pass of the pump light. For q-switching an acousto optic

modulator cut under Brewster angel was integrated in the resonator. Output couplers with transmissions from 3.8 % to 30 % were tested so far for cw and q-switched laser operation. Until now laser rods with doping concentrations of 0.5 % and 1 % were investigated. Figure 10 shows the laser output curves of a 62 mm long 0.5 % doped Ho:YAG rod for different output couplings on the left side. The highest output powers of up to 40 W were reached using 7 % output coupling. All curves show a drop of the holmium output power at an incident pump power of about 80 W because of the mentioned minimum in the absorption of Ho:YAG around 1895 nm (see fig. 8). The laser threshold is around 40 W and the maximum output power was achieved with 135 W of incident pump power on the crystal. This yields an optical to optical efficiency of about 33 %. The slope efficiency is about 40 % with respect to the incident pump power on the Ho:YAG crystal and 57 % with respect to the absorbed pump power. The 1 % doped crystal showed a slightly inferior performance. On the right side of figure 10 the best input output curve of a 1 % doped crystal is shown in comparison to the results of the 0.5 % doped crystal. The threshold of the 1 % doped crystal is higher (60 W) and the slope efficiency with respect to the absorbed pump power is nearly the same as for the lower doped crystal.
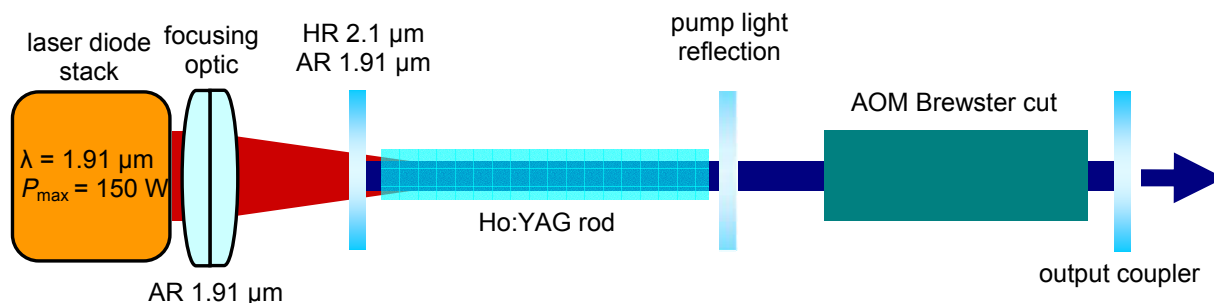

Fig. 9. Experimental set-up for the holmium laser experiments with q-switching

In recent experiments with the q-switched laser operation pulse energies up to 5 mJ were achieved with a pulse length of 180 ns. With an output coupling of 30 % the q-switched laser operated just above the laser threshold. The 5 mJ were observed for repetition rates of up to 250 Hz; at 1 kHz repetition rate only 3 mJ of pulse energy were observed.
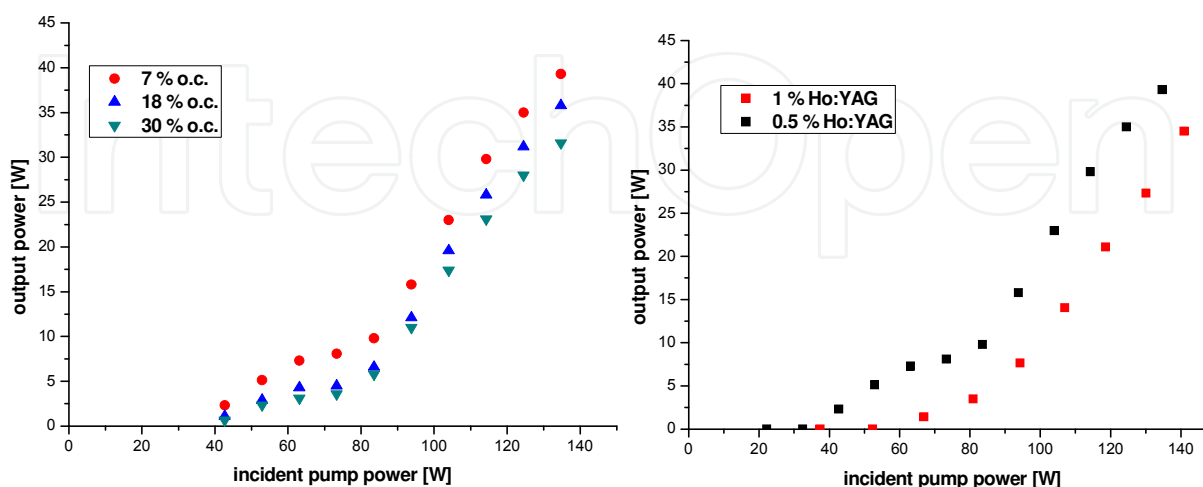

Fig. 10. Left side: Characteristic curves of a 0.5 % doped Ho:YAG rod with a length of 62mm for different output couplings (o.c.). Rigth side: Comparison of the output power for the 0.5 % and the 1 % doped crystal using 7 % o.c..

The presented results show the great potential of the in-band pumping of holmium crystals. Maximum cw output powers of up to 43 W and maximum pulse energies of up to 50 mJ were shown. The achieved slope efficiency 80 % with the fibre laser pumping shows that there are no significant upconversion losses for in-band pumping. The achieved results with the diode pumping demonstrated the feasibility of this sources for the pumping of Ho:YAG, but pumping Ho:YLF should also be possible with these diodes. In general the performances achieved with Ho:YLF and Ho:YAG are comparable. Further power scaling of the output powers should be possible with both systems when pump sources with higher powers become more easily available. A second option to achieve higher output powers is the realisation of multi stage amplifier systems.

3. GaSb-based diode laser systems around 2 µm

3.1 Laser diodes and diode stacks

In the last years great progress was made in the development of laser diodes emitting in the wavelength range around 2 µm. The efficiency and the output power could be significantly increased. Additionally the beam quality was improved (lower fast axis beam divergence) and the lifetime at room temperature operation was extended. Therefore these diodes can now address an increasing number of applications and they will become more and more commercially available. Depending on the emitted wavelengths and output powers one can use these compact and low-cost coherent sources for instance in gas sensing, free-space telecommunication, and medical applications or as pump sources for solid state laser systems. In principle GaSb-based laser diodes can be realised with emission wavelengths between 1.85 µm and 2.35 µm for room temperature operation (Rattunde et al., 2000).

In 1963 I. Melngailis demonstrated the first mid-infrared semiconductor laser based on the InAs material system (Melngailis, 1963). The laser operated at low temperatures and emitted light at 3.1 µm. The first room temperature mid-infrared laser was developed by Caneau et al. in 1985 (Caneau et al., 1985). This (GaInAsSb)(AlGaAsSb) double-heterostructure laser operated at 2.2 µm. Ten years later Baranov et al. reported on high temperature operation of the same semiconductor structures emitting at 2.1 µm (Baranov et al., 1994). All these systems delivered very low output powers, a breakthrough with respect to the upscaling of the laser output power for 2 µm diodes was achieved in 1992 (Choi et al., 1992). For the first time quantum-well-structured GaSb-based laser diodes were presented. This new design approach led to laser output powers up to 190 mW and it showed improved power exploitation in comparison with the mentioned double-heterostructures. From this invention it took about 10 years to achieve further power scaling of laser diodes that operate in the 2 µm wavelength range. The next invention to achieve higher output powers was a p-side down mounted broad-area GaSb-based laser diode (Rattunde et. al., 2002). The direct gap band-edge profile of a laser structure with an emission wavelength around 2 µm that was realised by Rattunde et al. is shown in figure 11. In such a diode, three compressively strained 10 nm thick $Ga_{0.78}In_{0.22}Sb$ quantum wells which are separated by 20 nm wide lattice matched $Al_{0.29}Ga_{0.71}As_{0.02}Sb_{0.98}$ barriers compose the active region. The active region itself is located between two 400 nm thick $Al_{0.29}Ga_{0.71}As_{0.02}Sb_{0.98}$ confinement layers which were sandwiched between 2.0 mm wide lattice matched $Al_{0.84}Ga_{0.16}As_{0.06}Sb_{0.94}$ n- and p-doped cladding layers.

Due to the broad area the differential and thermal resistance of this laser was reduced. This provided a maximum output power of up to 1.7 W at room temperature. The great potential

of this semiconductor material system was recognised instantly and Shterengas et al. soon fabricated the first linear array with this type of diodes (Shterengas et. al., 2004). Linear laser arrays on a 1-cm-wide bar with 19 100 µm wide emitters and 1-mm-long cavities were built and characterised. With this first high-power diode laser linear array 10 W of output power at 2.3 µm were achieved for continuous wave laser operation at room temperature. The spectral width of the linear array output was about 20 nm and the achieved peak wall-plug efficiency was already near 9 %. But these first high power diodes and bars had one big disadvantage, which was the large fast axis beam divergence. This large divergence of 67° FWHM results from the broad-area design of the diode laser and it considerably limits the applications for this type of diodes. With this large divergence fibre coupling is extremely difficult and also the practical use as a pumping source for solid state lasers requires a FWHM ≤ 45° in order to collimate the emitted beam of the laser diodes with state-of-the-art collection optics.
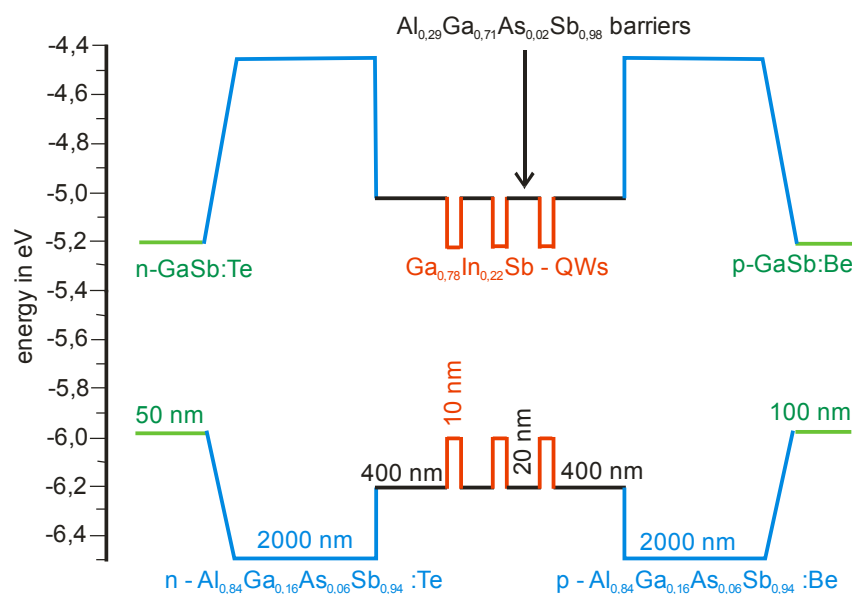

Fig. 11. Direct gap band-edge profile of a broad area GaSb-based laser diode with an emission wavelength of 2 µm (Rattunde et. al., 2006a)

In 2006 Rattunde et al. achieved a significant reduction of the beam divergence of the GaSb-based diodes by applying an improved waveguide design. A comparison between the fast axis far field beam profiles of the new narrow waveguide design diodes and the conventional designed diodes is shown in figure 12. With the new design the fast axis divergence was reduced to 44° FWHM, furthermore an excellent slow axis beam quality was achieved (Rattunde et al., 2006b). The newly designed laser diodes exhibited a maximum cw output power of 1.96 W at a wavelength of 2.0 µm.

In 2006 Kelemen et al. developed and characterised high-power 1.91 µm (AlGaIn)(GaSb) quantum-well diode laser single emitters and linear arrays with the new narrow waveguide design (Kelemen et al., 2006). A single emitter showed a maximum output power of nearly 2 W with a slope efficiency of 0.32 W/A at room temperature. The 1-cm-long tested linear array consisted of 19 emitters. The maximum cw output power of this bar was limited to 16.9 W by the thermal rollover. The slope efficiency of the bar was about 0.31 W/A and the maximum wall plug efficiency was 26 %. The wavelength shift of the bar was measured to be 1.4 nm/K and 1.2 nm/W, so the thermal shift and the shift on power dissipation are slightly higher than for a single emitter (1.2 nm/K and 8.6 nm/W).
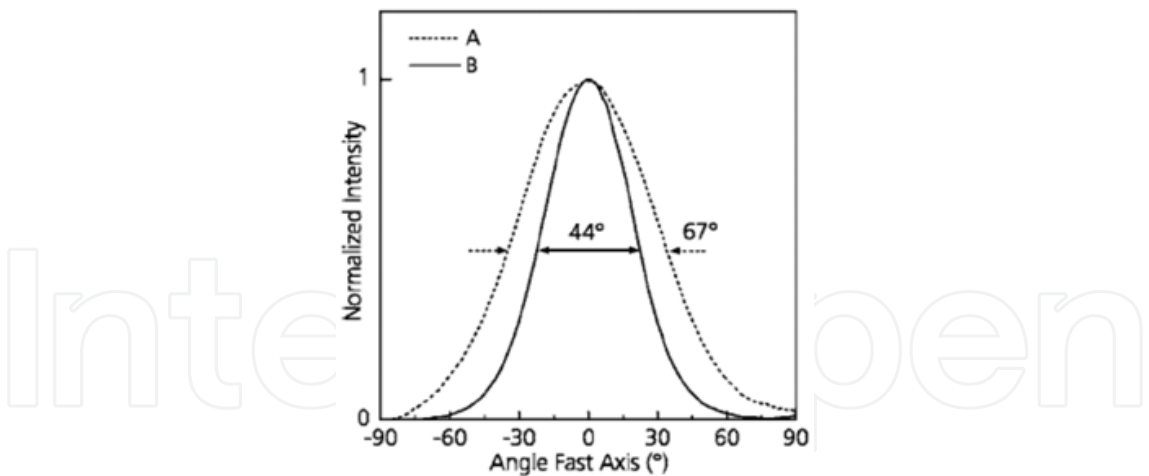
Fig. 12. Measured fast axis far-field beam profiles of a broad area diode (doted line) and a diode with reduced beam divergence (continuous line) (Rattunde et al., 2006b)

In 2007 LISA laser products OHG bought a high power multi-bar stack that was build with ten linear arrays of the type that was characterised and described by Kelemen et al. before. This first GaSb-based diode stack is directly water cooled and integrated into a sealed housing. The single emitters used have a stripe-width of 150 μm and a pitch of 500 μm. The rear facets are coated with a highly reflective double-stack of Si and SiO_2 films (> 95 % reflectivity) and the front facets are coated by a single layer of SiN (3 % reflectivity). The emitters were collimated only in the fast axis with micro optics which are integrated in the sealed housing. The used waveguide concept which leads to a low fast axis beam divergence of 44° FWHM allows a collimation with common pumping diode optics. In order to focus the emitted beam of the laser diode stack into a laser crystal the remaining slow axis divergence has to be compensated with a cylindrical lens.

Important aspects for the holmium pumping are the current-power characteristic, output spectra and the spectral shift of the laser diode stack. Figure 13 shows the current-power characteristic at a cooling temperature of 15 °C for continuous wave operation on the left side and the shift of the central wavelength with respect to the output power of the diode stack on the right side.
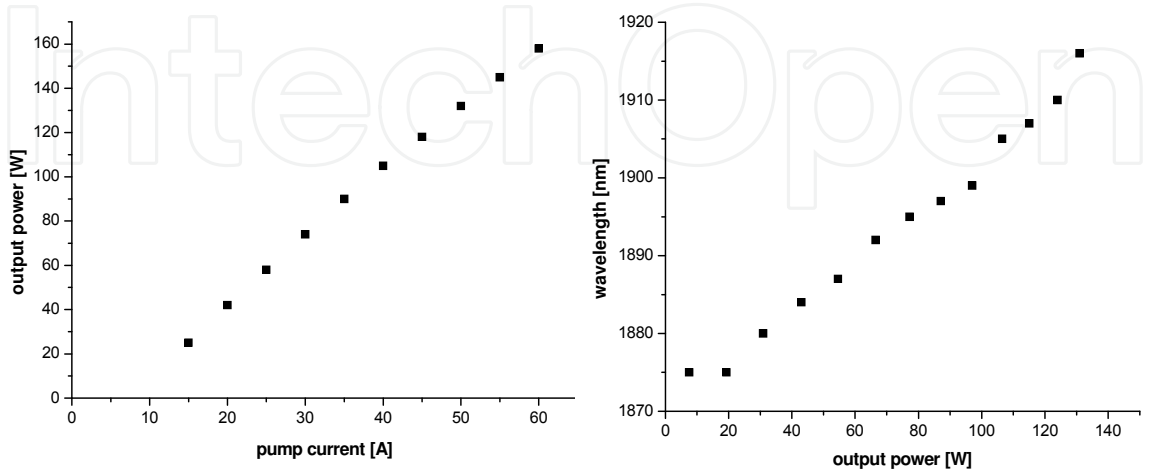

Fig. 13. Left diagram: Characteristic curve of the GaSb multi-bar stack at 15 °C. Right diagram: Shift of the central wavelength with respect to the output power.

The threshold current of the laser diode stack is 8 A and the maximum continuous wave output power is 158 W leading to a slope efficiency of 2.95 W/A. The right side of figure 13 shows that the central wavelengths of the laser diode stack shifts over 40 nm from laser threshold to the maximum output power (0.26 nm/W). This large wavelength shift is a significant disadvantage for the pumping of holmium lasers, since the absorption of holmium ions in most host crystals changes dramatically over this wavelength range. One can see in figure 8 that the main absorption peak of Ho:YAG at 1910 nm has a line width of only 7 nm and also Ho:YLF has a line width of only about 15 nm at the absorption maximum around 1940 nm.

An additional problem of the laser diode stack is the very broad emission spectrum. In figure 14 the emission spectra of the laser diode stack at different pump powers (left side) and an output spectrum of a single emitter (right side) are shown. Each spectrum is normalised. On the left side one can see that the emission of the diode stack shifts to longer wavelengths with higher pumping currents and in addition, the structure of the spectrum becomes more inhomogeneous. This effect causes the broadening of the emission spectrum with higher pumping currents from 8 nm to 20 nm.
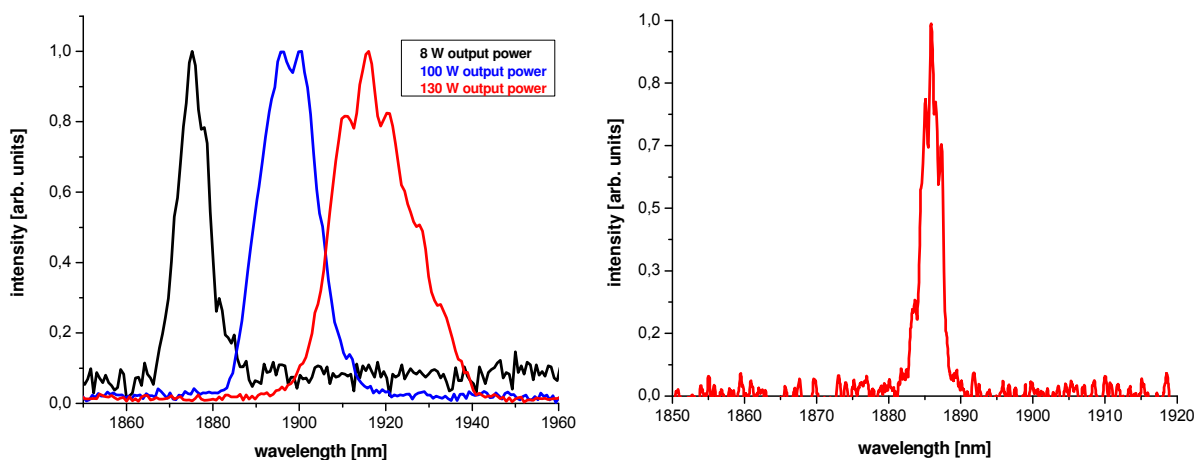

Fig. 14. Left side: Normalised output spectra of the diode stack for different output powers. Right side: Output spectrum of a single emitter at low output power.

Due to the big improvements of the GaSb-based diodes in the recent years these laser sources have now become interesting for many purposes. Current research and development therefore focuses on the optimisation of these lasers towards specific applications. Single emitters can be used as cheap sources for sensing or spectroscopy. Using external resonators single-mode cw operation can be realised with the diodes, which makes it possible to use them as seed sources for high power lasers (Jacobs et al., 2004). As shown in section 2, laser bars or stacks can be used for solid state laser pumping. But these lasers become also interesting for other industrial or medical applications, especially when the efficiency and the beam quality can be further increased. Nowadays GaSb-based diodes are becoming commercially available, for instance by m2k Laser.

3.2 Optically pumped GaSb-based semiconductor disk lasers

The poor spatial quality of the output of conventional GaSb-based 2 μm laser diodes limits their applications. Using a different design for the semiconductor and optical pumping, a very high brightness can be achieved. Optically pumped semiconductor disc lasers (OPSDL)

also known as vertical-external-cavity surface emitting lasers (VECSEL) are optically pumped similar to solid state thin disc lasers (Kuznetsov et al., 1997). The OPSDL chip, formed by a sequence of epitaxially grown semiconductor layers, simultaneously acts as the cavity mirror and the gain region. A pump laser is focused onto the surface of the chip with a spot-size typically several tens or hundreds of microns in diameter. To complete the laser resonator an arrangement of external mirrors and other components is used. A typical OPSDL set-up with a two mirror cavity is shown on the left side of figure 15. To achieve optimal cooling of the OPSDL chip a heat-spreader is often mounted on the surface (Schulz et al., 2008). A typical OPSDL structure with heat-spreader and the heat flow is shown on the right side of figure 15. The OPDSDL design offers several advantages: The emission wavelength can be varied by the design of the OPSDL structure in the same way as for conventional semiconductor lasers. Mode matching of pump and laser beam by variation of the external resonator design often provides diffraction limited output beams. The external resonator also allows flexible control of the laser properties by the insertion of intra-cavity elements like frequency stabilization, passive mode-locking, or frequency doubling.
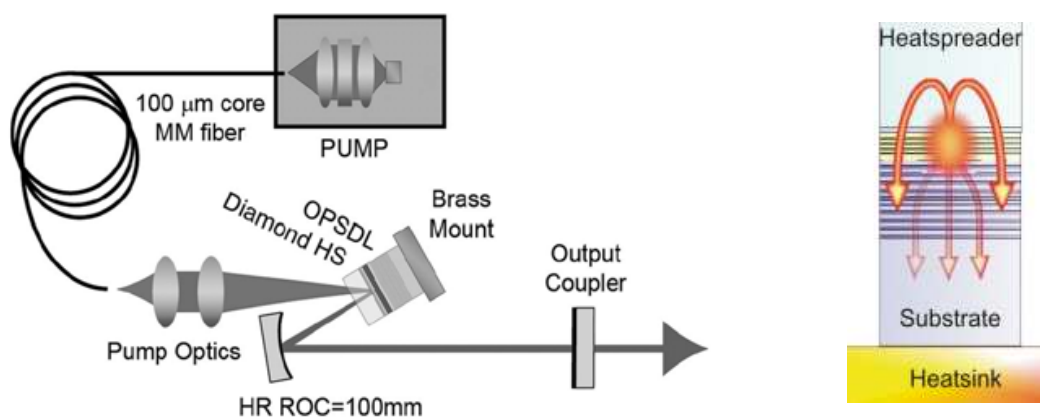

Fig. 15. Schematic set-up of an OPSDL with a folded external cavity (left side) and the heat flow in an OPSDL with a heat-spreader (right side) (Schulz et al. 2008).

GaSb-based OPSDLs can be realised within the wavelength range from 2.0 µm to 2.5 µm. In the 2 µm wavelength range either SiC or diamond are used as heat-spreader. Due to the lower thermal conductivity of SiC the output powers of lasers with SiC heat-spreaders are lower than for diamond ones. On the left side of figure 16 typical input-output curves of an GaSb-based OPSDL with a SiC heat-spreader emitting at 2020 nm are shown for different cooling temperatures. As a pump source a commercial fibre coupled laser diode emitting at 976 nm and a resonator similar to the one shown in figure 15 with about 4 % output coupling was used. The maximum output power of this laser was 2.5 W at 9 °C and 2.0 W at 18 °C. The strong temperature dependence is a result of the high heat load in the chip caused by the large quantum defect between the pump and the laser wavelength. The highest output powers of up to 5 W were achieved with GaSb-based OPSDLs operating at 2.0 µm using a diamond heat-spreader (Hopkins et al., (2008). At longer wavelengths the maximum output powers are lower so far.

By integrating a quartz birefringent filter into the collimated arm of the folded resonator, wavelength tuning and single mode laser operation can be achieved. With an 8 mm thick quartz birefringent filter a maximum single mode output of 0.8 W at 2005 nm with an OPSDL chip with a SiC heatspreader were achieved. On the right side of figure 16 the

maximum single mode output powers achieved with this chip for different wavelengths are shown. The large wavelength tuning was achieved using the birefringent filter and the variation of the pump power for wavelength tuning. The wavelengths tuning was not continuously due to the etalon effect of the uncoated SiC heatspreader used in this experiment. The highest tuning range achieved with a birefringent filter and single mode laser operation of a GaSb-based OPSDL was 70 nm around 2.3 µm (Hopkins et al., 2007). An OPSDL with a diamond heat spreader was used which reached a maximum single mode output power of 860 mW when cooled to -15 °C. Stable single-mode laser operation of an OPSDL could also be demonstrated by using a volume Bragg grating (VBG) as output coupler (Scholle et al., 2009). Up to 0.8 W were achieved at 2013 nm by using the VBG with about 98 % reflectivity as output coupler.
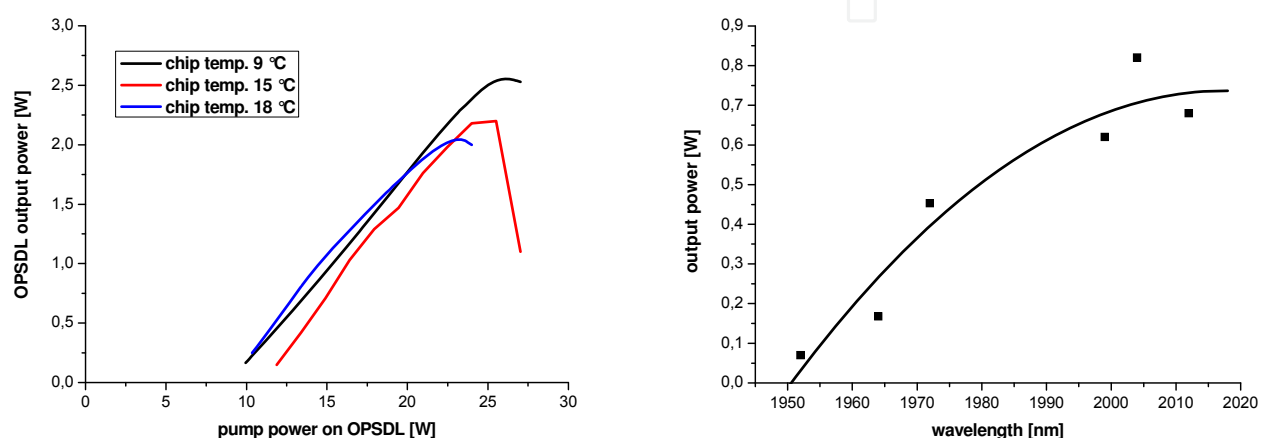

Fig. 16. Input-output curve of a GaSb-based OPSDL with a SiC heatspreader (left side) and maximum single mode output of this OPSDL achieved with a birefringent filter for different wavelengths (right side).

OPSDL combine some of the biggest advantages of semiconductor and solid state lasers. They can be designed for different wavelengths like semiconductor lasers and they can provide high beam qualities like solid state lasers. This makes OPSDLs attractive for a wide spectrum of applications. Until now the maximum output powers of GaSb-based OPSDLs are quite low, but they can be increased in the future. The possibility of wavelength selection and single mode operation makes OPSDLs an ideal seed source for secondary amplifier or laser stages. The major disadvantage for OPSDLs is the lack of energy storage due to the short carrier lifetimes.

4. Most attractive laser applications in the 2 µm wavelength range

4.1 Laser sensing and spectroscopy
The 2 µm wavelength range is called "eye safe", since laser radiation of this wavelength is absorbed in the vitreous body of the eye and does not reach the retina. Therefore the threshold for untreatable eye damage is much higher than for shorter wavelengths. Laser systems that operate in the "eye safe" wavelength range have great market potential especially in free space applications where eye safety is very important. So these laser systems are ideal for the usage in LIDAR (LIght Detection And Ranging) systems. LIDAR systems operate very similar to radar systems except that aerosol particles suspended in the air provide the return signal.

In the wavelength range at 2 μm there are absorption lines of a number of atmospheric gasses (e.g. H_2O, CO_2, N_2O) which can be detected and analysed in this spectral region. There are different detection techniques for chemical sensing based on short, medium and long detection paths. Short range detection means in the immediate location of the laser system and the detector, often with both in the same compact housing. Medium range refers to a short open path between the source and the detector (some metres). This includes systems with an integrated measurement system that use a multi-pass Heriotstyle cell or chamber containing the gas of interest. Long range here refers to any detection made over an appreciable distance (100 m to several km). These systems use the backscattered light for the measurement. To gain position and direction information, pulsed sources of appreciable energy are required for long range detection. In the 2 μm wavelength range there are many atmospheric transmission windows where very long detection ranges can be realised.

One of the key technologies opened up by tunable laser sources in the 2 μm region is the sensitive detection of some lighter atmospheric gasses and molecules. For this type of detection there are a number of lower power cw techniques appropriate. Most of these rely on differential optical absorption spectroscopy DOAS (Platt & Stutz, 2008). The systems detect a specific gas by exploiting the specific absorption of the gas at some wavelength. The backscattered light at this wavelength is compared with the level of returned light at another to confirm the presence of the gas of interest while eliminating other potential contaminants. In most cases, it is reasonable to compare the absorption of the species of interest with a known absorption line of another species like water vapour for example. There are many methods of detection with varying complexity and suitability for different applications; many of these employ a tunable source to allow the probe wavelength to scan through the wavelengths of interest. Remote chemical sensing with compact and robust laser sources in the 2 μm wavelength range has good potential in the chemical and petroleum industries in terms of safety, quality control, and regulatory enforcement as well as in medical and environmental applications. Recently the sensing of a number of chemical markers in breath analysis (such as ammonia - NH_3) has been shown to provide early diagnosis of chronic medical conditions.

The wind velocity can be measured using a Doppler-LIDAR system which operates with heterodyne detection. Aerosol particles travel essentially as fast as the surrounding air. When they scatter the incident laser radiation, they impart a slight Doppler shift to the returning radiation. Using heterodyne detection, the Doppler shift can be measured and thus the wind velocity at the place of the scattering can be determined. To achieve high detection ranges and high resolutions most of the Doppler-LIDAR systems are realised in a master oscillator – power amplifier (MOPA) configuration. A low-power narrow line width master laser with a fixed or tunable wavelength is used to seed a high power laser that adopts the characteristics of the master laser. A high short-term stability of the laser frequency is necessary to reach a high resolution for the wind velocity measurement. At a wavelength of 2.0 μm a resolution of 1 m/s of the wind velocity can be reached only when the frequency stability of the laser is better than 1 MHz.

Ground-based 2 μm Doppler-LIDAR systems can be used at airports to detect wake vortex formation during take-off and landing of aircraft to improve the safety. In the European project I-WAKE (Instrumentation system for on-board wake vortex and other hazards detection, warning and avoidance) a thulium solid state laser based 2 μm MOPA system was developed for an eye safe air-borne Doppler-LIDAR. The goal of the system was to

detect wake-vortex formation during approach and landing and to detect wind shear and clear-air turbulences during the flight to increase the capacities of the airports and the flight safety (I-WAKE, 2001).

4.2 Medical applications

There are several aspects which make the 2 µm wavelength range a promising candidate for highly precise surgical applications for both soft and hard tissue. The most important property is the high absorption in water combined with minimal penetration depth within human tissue. The superficial mid-infrared tissue ablation effects lead to submicron ablation rates which result in minimal damage around the exposed area. The second important aspect is the coagulation effect caused by the 2 µm laser radiation, which suppresses the bleeding during operations. In the most cases, solid state lasers are used for well established medical procedures such as precise tissue ablation, ophthalmic surgery or dentistry. Figure 18 shows the main medical applications and their anatomic regions within the whole human body. For the applications printed in red pulsed laser systems are used, for the others cw laser radiation is more practical.
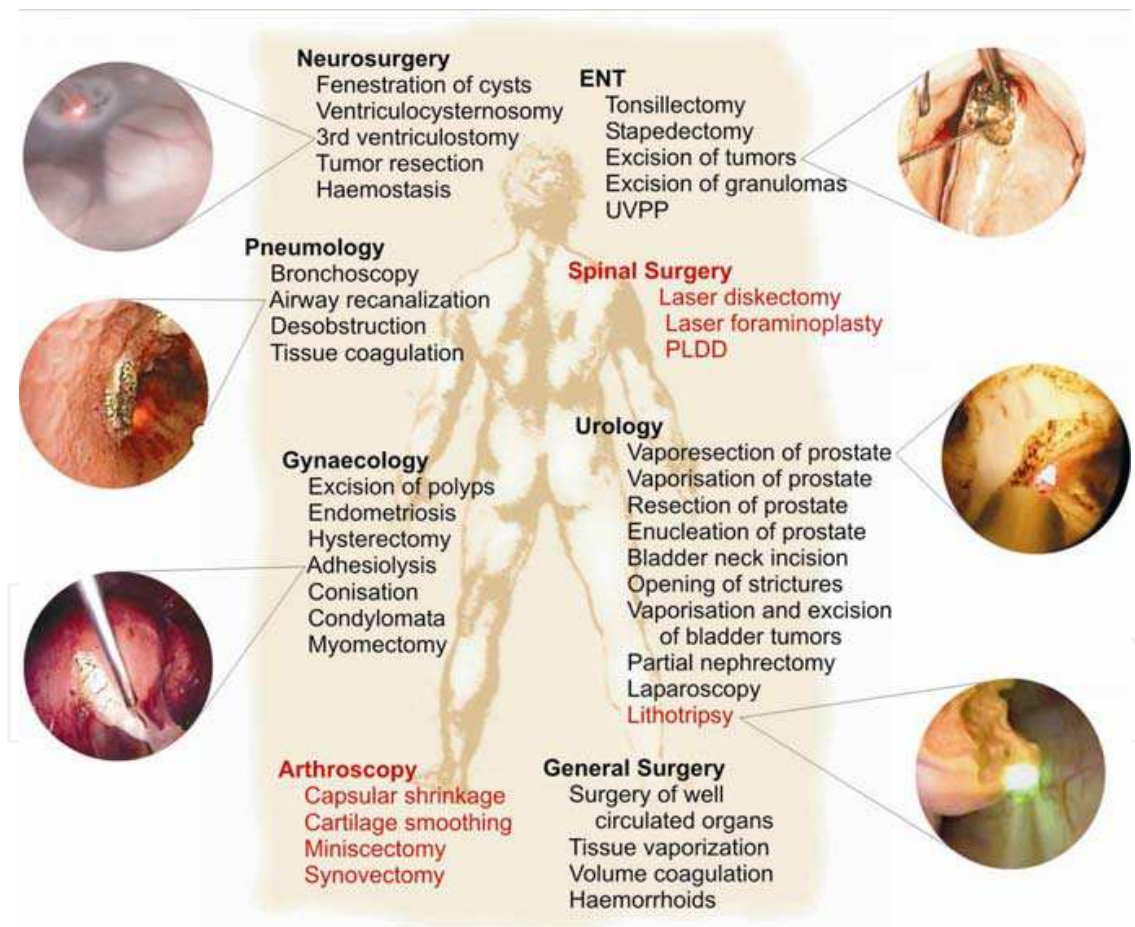

Fig. 18. Overview with key-hole pictures of different possible surgery operations which can be carried out with laser systems operating in the 2 µm wavelength range. For the applications marked in red pulsed laser systems are used.

Depending on the diagnostic findings and the sort of therapy, most of the medical procedures are carried out either with a Ho:YAG laser or Tm:YAG laser systems because of

the penetration depth and the already mentioned absorption of this specific laser radiation in water. The Ho:YAG laser operates at 2.1 μm and the Tm:YAG laser operates at 2 μm. Although their wavelengths are close-by their penetration depths distinguish clearly. In soft tissue the Ho:YAG laser has a penetration depth of 300 μm and the Tm:YAG laser penetrates only 100 μm. There are four fundamental photoablation mechanisms which cause these differences depending on the wavelength: photochemical processes, photothermal processes, photomechanical processes and photoelectrical processes. The first type describes laser stimulation effects on biochemical and molecular interactions. The second mechanism is the actual photoablation. The tissue is removed by vaporization and superheating of tissue fluids. The photomechanical process breaks apart the tissue structures and leads to tissue removal by laser-induced shock-wave generation. The fourth mechanism, the photoelectrical process, achieves tissue removal by electrically charged ions and particles.

The first laser lithotripsy was reported in 1981 (Orii et al., 1981). A cw Nd:YAG laser emitting at 1.064 μm was used to successfully clear pigmented common bile duct (CBD) stones from humans. A big drawback of this wavelength is the strong generation of wall heat which leads to damage of the bile ducts. Therefore many investigations were carried out characterising other laser wavelengths. The pulsed dye laser operating at 504 nm gained in importance and led to many successful interventions, but nevertheless did not become widely accepted because of its limited range of applications and high costs. Today, interventions made by Ho:YAG laser systems show complete stone fragmentation in over 90 % of all lithotripsies and the stones of all compositions can be reduced better than with other laser wavelengths (Teichman et al. 2001). In the case of the Ho:YAG laser the power required for lithotripsy is the same for all stones. In contrast, the required laser power of the dye laser had to be changed substantially among different stone compositions. The reason is that the fragmentation by Ho:YAG lithotripsy is caused primarily by photothermal mechanism which transfers the laser energy directly to the stone. Therefore potentially hazardous cavitation bubbles or shock waves are not caused by the Ho:YAG laser. Teichman et al. also investigated the potential of the lithotripsy of gallstones by a Ho:YAG laser system. The laser energy was guided endoscopically by a fibre to the targeted stones. They conclude that Ho:YAG laser lithotripsy is effective and safe when used to fragment gallstones.

In a study Bach discusses about the feasibility and efficacy of a Tm:YAG laser system (RevoLix, LISA laser products OHG, Germany) for prostatectomy (Bach et al. 2009). Three surgeons used the 70-W 2-μm cw Tm:YAG laser system which was coupled with a 550 μm core fibre for the intervention of 208 patients. The study showed that the Tm:YAG laser assisted prostatectomy is feasible and effective, even in patients with potentially impaired detrusor function.

4.3 Material processing

The 2 μm wavelength range is also very attractive for material processing especially for plastics. The most interesting aspect is the processing of plastic materials that are transparent in the visible wavelength range. Figure 19 shows a schematic diagram of the welding process for two transparent plastics and two pictures of plastic welds prepared with a thulium 2 μm laser. Most of the relevant plastic materials show sufficient absorption around 2.0 μm to allow direct processing with lasers operating at this wavelength. Using the absorbed energy of a 2.0 μm laser cutting, welding, and marking are easily possible. Using

"standard" 1 µm lasers this is only possible with additives inside the plastic that increase the absorption of the laser light, because the plastics are still highly transparent in this wavelength range. These additives make the fabrication process more complicated and the addition is sometimes prohibited for example when the plastics are used in medical applications. Laser systems for such applications have to deliver high cw output powers with a good beam quality and they have to be highly reliable for industrial operation. Possible applications in this field also include the processing and fabrication of transparent bio-fluidic chips (precise welding or generating of micro-channels) for biological or medical mass-screening experiments.
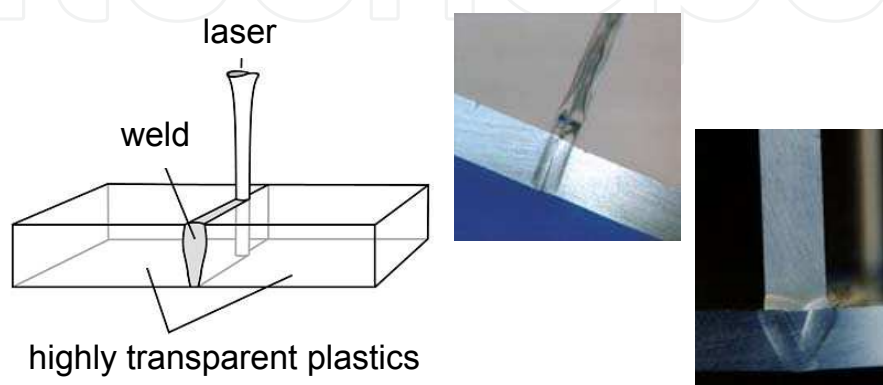

Fig. 19. Left side: Schematic diagram for welding two highly transparent plastics with a butt joint. Right side: Welding examples prepared with a 2 µm Tm:YAG laser by Prolas GmbH, Aachen (butt joint 4 mm PMMA and T-bonding 3 mm PMMA)

4.4 Further possibilities

Besides the described applications 2 µm laser systems are also interesting for free space optical (FSO) communication, military and security applications and for pumping of laser sources for the mid infra-red region. FSO communication solutions are used for low-cost metro networks. Suitably robust and cheap laser systems working at emission wavelengths in the first water absorption window at 2 µm are attractive for these systems. Due to the eye safe wavelength higher powers can be used as at 1 µm and long ranges can be achieved for operation at an atmospheric transmission window. Combined with the availability of small area fast detectors, this offers real prospects for such systems.

There are a number of security and military applications for 2 µm laser systems with different requirements on the brightness, compactness or cost-effectiveness of the systems. While many heavier elements and more complex explosive compounds (TNT, TATP) and chemo-biological agents (Sarin, Soman) may be directly detected at longer wavelength ranges (7 to 9 and 9 to 12 µm respectively) it is worth noting that the presence of explosives may be betrayed by increased levels of lighter constituent compounds or 'markers' either through out gassing or decomposition or residue from manufacture (such as ammonia or acetone), which can be detected at a wavelength of 2 µm (Day et al., 2007). For instance, current airport swab spot checks look for residue markers – this could be done remotely and passively with a photonic chemical sensor providing mass throughput screening. Detecting chemical and biological warfare agents and related solvents is obviously of increasing importance for ensuring public and armed-forces safety.

Another potential application in the security context is the deployment of secure short-range communication networks on a battlefield. This can be well achieved at eye-safe wavelengths within an atmospheric transmission window. Here it is advantageous to provide low-power, tunable, and pulsed operation from the source to ensure covert, spread-spectrum communications with little backscattered or dispersed light out of the line-of-sight path, therefore ensuring secrecy and security.

$2\,\mu m$ laser systems are also ideal pump sources for laser systems that emit at longer wavelengths in the mid-infrared. Especially the pumping of Cr^{2+} lasers and optical parametric oscillators (OPOs) is of interest. Cr^{2+} lasers can be pumped and operated continuously and they are broadly tunable. They can cover the whole wavelength range from 2000 nm to 3100 nm (Sorokina & Vodopyanov, 2003). Efficient pumping of Cr2+ lasers has already been demonstrated with diode lasers and thulium lasers. OPOs allow broad continuous wavelength tuning, high peak powers, and high conversion efficiencies. They use a nonlinear optical frequency down-conversion mechanism in which one pump photon decays into two photons with lower energy (longer wavelength). The sum of the energies of the two new photons is equal to the energy of the pump photon. The two new photons do not have the same energy; typically the photon with the higher energies is called "signal" and the other one "idler". For high power applications in the mid-infrared, usually OPOs based on ZGP are used. ZGP OPOs can ideally be pumped with holmium lasers around $2.1\,\mu m$ (Budni et al. 1998; Vodopyanov, 2003).

5. Conclusion

In this chapter the recent progress in the development of crystal lasers, fibre lasers and semiconductor lasers operating in the wavelength range close to $2\,\mu m$ are discussed. For the crystal and fibre lasers the focus is put on the improvements, developments, and recently achieved high power laser results of thulium and holmium doped systems. Thulium laser systems emitting around $2.0\,\mu m$ can be pumped very efficient nearby 800 nm, when the cross relaxation process, which populates the upper laser level, is exploited very well. Output powers close to $1\,kW$ and slope efficiencies of up to 68 % have recently been reported. Concerning the holmium laser systems the most recently achieved results for inband pumping at $1.9\,\mu m$ with different sources are reviewed and discussed. Using inband pumping q-switched pulses of up to 55 mJ of pulse energy and of 43 W of cw output power have been demonstrated.

Additionally the latest improvements of GaSb-based laser diodes and stacks are outlined. These diodes can cover the whole wavelength range from $1.85\,\mu m$ to $2.35\,\mu m$ and they get more and more commercially available. The potential of efficient holmium pumping with a diode stack is shown.

In the last section the potential applications for the different $2\,\mu m$ laser sources are presented. Applications in spectroscopy, sensing, surgery, and material processing are discussed in detail.
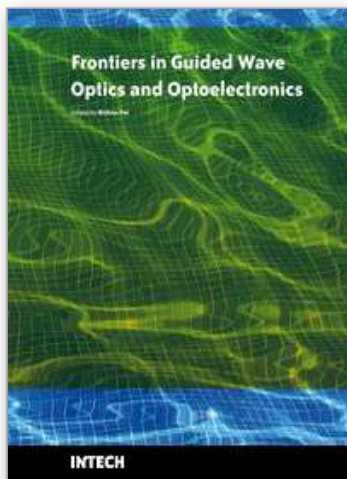
6. References

Agger, S. D. & Povlsen, J. H. (2006). Emission and absorption cross section of thulium doped silica fibers, *Opt. Express,* Vol. 14, No. 1, pp. 50-57

Bach, T.; Herrmann, T. R. W.; Haecker, A.; Michel, M. S. & Gross, A. (2009). Thulium:yttrium-aluminium-garnet laser prostatectomy in men with refractory urinary retention, *BJU International,* Vol. 104, No. 3

Baranov, A. N.; Fouillant, C.; Grunberg, P.; Lazzari, J. L.; Gaillard, S. & Joullié, A. (1994). High temperature operation of GaInAsSb/AlGaAsSb double-heterostructure lasers emitting near 2.1 µm, *Appl. Phys. Lett.*, Vol. 65, 5

Becker, T.; Clausen, R. & Huber, G. (1989). Spectroscopic and Laser Properties of Tm-doped YAG at 2 µm. *OSA Proceedings on Tunable Solid-State Lasers,* 5, 150

Bollig, C.; Strauss, H. J.; Esser, M. J. D.; Koen, W.; Schellhorn, M.; Preussler, D.; Nyangaza, K.; Jacobs, C.; Bernhardi, E. H. & Botha, L. R. (2009). Compact Fibre-Laser-Pumped Ho:YLF Oscillator-Amplifier System, *CLEO EUROPE 2009*

Budni, P. A.; Pomeranz, L. A.; Lemons, M. L.; Schunemann, P. G.; Pollak, T. M. & Chicklis, E. P. (1998). 10 W mid-IR holmium pumped $ZnGeP_2$ OPO, *Advanced Solid State Lasers, Tech. Digest,* Opt. Soc. Am., Washington, DC, pp. 90-92

Budni, P. A.; Lemons, M. L.; Mosto, J. R. & Chicklis, E. P. (2000). High-Power/High-Brightness Diode-Pumped 1.9-µm Thulium and Resonantly Pumped 2.1-µm Holmium Lasers, *IEEE J. of Selected Top. In Quant. Electr.,* Vol. 6, No. 4, pp. 629634

Budni, P. A.; Ibach, C. R.; Setzler, S. D.; Gustafson, E. J.; Castro, R. T. & Chicklis, E. P. (2003). 50-mJ, Q-switched, 2.09-µm holmium laser resonantly pumped by a diode-pumped 1.9-µm thulium laser, *Optics Letters,* Vol. 28, No. 12, pp. 1016-1018

Caird, J. A.; DeShazer, L. G. & Nella, J. (1975). Characteristics of room-temperature 2.3-µm laser emission from Tm^{3+} in YAG and YALO$_3$. *IEEE J. Quantum Electron.*, 11

Caneau, C.; Srivastava, A. K.; Dentai, A. G.; Zyskind, J. L. & Pollack, M. A. (1985). Room-temperature GaInAsSb/AlGaAsSb DH injection lasers at 2.2 µm, *Electron. Lett.*, Vol. 21, p 815

Chicklis, E. P.; Naiman, C. S., Folweile, R. C.; Gabbe, D. R.; Jenssen, H. P. & Linz, A. (1971). High-Efficiency Room-Temperature 2.06-MUM Laser Using Sentitized HO3+-YLF, *Appl. Phys. Lett*, 19, 4

Choi, H. K. & Eglash, S. J. (1992). High-power multiple-quantum-well GaInAsSb/AlGaAsSb diode lasers emitting at 2.1 µm with low threshold current density, *Appl. Phys. Lett.*, Vol. 61, 10

Day, T.; Pushkarsky, M.; Weida, M.; Arnone, D. & Pritchett, R. (2007). Miniaturized, Tunable, External Cavity Quantum Cascade Lasers, *8th International Conference on Mid-Infrared Optoelectronics: Materials and Devices (MIOMD-VIII),* Bad Ischl, Austria

Dergachev, A.; Moulton, P. F. & Drake, T. E. (2005). High-power, high-energy Ho:YLF laser pumped with Tm:fiber laser, *Advaced Solid State Photonics 2005* (The Optical Society of America, Washington, DC, 2005), post-deadline paper SS1-6

Duczynski, E. W.; Huber, G.; Ostroumov, V. G. & Shcherbakov, I. A. (1986). Cw double cross pumping of the $^5I_7$-$^5I_8$ laser transition in Ho^{3+}-doped garnets, *Appl. Phys. Lett.*, 48, 23, pp. 1562-1563

Ermeneux, F. S.; Sun, Y.; Cone, R. L.; Equall, R. W.; Hutchenson, R. L. & Moncorge, R. (1999). Efficient cw 2 µm Tm^{3+}:Y_2O_3 Laser, *Adv. Solid-State Lasers,* Vol. 26, pp. 497-502

Fan, T. Y.; Huber, G.; Byer, R. L. & Mitzscherlich, P. (1987). Continuous-wave operation at 2.1 µm of a diode-laser-pumped, Tm-sensitized Ho:$Y_3Al_5O_{12}$ laser at 300 K, *Optics Lett.*, Vol. 12, No. 9, pp 678-679

Fan, T. Y.; Huber, G.; Byer, R. L. & Mitzscherlich, P. (1988). Spectroscopy and Diode Laser-Pumped Operation of Tm, Ho:YAG. *IEEE J. Quantum Electro.*, 24, 6

Fornasiero, L.; Berner, N.; Dicks, B.-M.; Mix, E.; Peters, V.; Petermann, K. & Huber, G. (1999). Broadly tunable Laseremission from Tm:Y_2O_3 and Tm:Sc_2O_3 at 2μm, *Conference on Advanced Solid-State Lasers, OSA Technical Digest,* paper WD5

French, V. A.; Petrin, R. R.; Powell, R. C. & Kotka, M. (1992). Energy-transfer processes in Y3Al5O12:Tm,Ho, *Phys. Rev. B,* 46, p. 8018

Frith, G. P., Samson, B., Carter, A. Farroni, J. & Tankala, K. (2007). Highpower (110), high efficiency (55%) FBG fibre laser operating at 2 μm, Proc. SPIE 6453, 64532B

Gaumé, R.; Viana, B; Vivien, D.; Roger, J.-P. & Furnier, D. (2003). A simple model for the prediction of thermal conductivity in pure and doped insulating crystals, *Appl. Phys. Lett.,* Vol. 83, No.7, p.1355

Heine, F. (1995). Diodengepumpte Festkörperlaser für Kommunikationstechnologie und Fernerkundung, *Dissertation,* Institut für Laser-Physik, Universität Hamburg

Honea, E. C.; Beach, R. J.; Sutton, S. B.; Speth, J. A.; Mitchell, S. C.; Skidmore, J. A.; Emanuel, M. A. & Payne, S. A. (1997). 115-W Tm:YAG Diode-Pumped Solid-State Laser. *IEEE J. of Quant. Electr.,* Vol. 33, No. 9, pp. 1592-1600

Hopkins, J.-M.; Hempler, N.; Rösener, N.; Schulz, N.; Rattunde, M.; Manz, C.; Köhler, K.; Wagner, J. & Burns, D. (2008). High-Power, (AlGaIn)(AsSb) semiconductor disk laser at 2.0 μm, *Opt. Lett.,* Vol. 38, No. 2, pp. 201-203

Huber, G.; Duczynski, E. W. & Petermann, K. (1988). Laser pumping of Ho-, Tm-, Er-doped garnet lasers at room temperature, *IEEE J. Quantum Electro.,* 24, pp. 924-933

I-WAKE Consortium (2001). Instrumentation systems for on-board WAKE-vortex and other hazards detection warning and avoidance. *DOW, Growth Project GRD1-2001-4076*

Jacobs, U. H., Scholle, K., Heumann, E., Huber, G. Rattunde, M. & Wagner, J. (2004). Room-temperature external cavity GaSb-based diode laser around 2.13 mm, *Appl. Phys. Lett.,* Vol. 85, No.4, pp. 5825-5826

Johnson, L. F. (1963). Optical maser characteristics of rare-earth ions in crystals, *J. Appl. Phys.,* 34, pp. 897-909

Johnson, L. F.; Geusic, J. E.; & Uitert, L. G. V. (1965). Coherent oscillations from Tm^{3+}, Ho^{3+}, Yb^{3+} and Er^{3+} ions in yttrium aluminum garnet, *Appl. Phys. Letters,* 7 (5), 127

Johnson, L. F.; Geusic, J. E. & Uitert, L. G. V. (1966). Efficient, high-power coherent emission from Ho3+ ions in yttrium aluminum garnet, assisted by energy transfer. *Appl. Phys. Letters* 8, 200

Kaminskii, A. A. (1996). Crystalline Lasers: Physical Processes and Operating Schemes, *CRC Press*, 978-0849337208, Boca Raton

Kelemen, M. T.; Weber, J.; Ratunde, M.; Kaufel, G.; Schmitz, J.; Moritz, R.; Mikulla, M. & Wagner, J. (2006). High-Power 1.9-μm Diode Laser Arrays With Reduced Far-Field Angle, *IEEE Photonics Technology Letters*, 18, 4

Kintz, G. J.; Esterowitz, L. & Allen, R. (1987). Cw diode-pumped Tm3+:YAG 2.1μm room-temperature laser *Electr. Lett.,* Vol. 23, No. 12, p. 616

Koechner, W. (2006). Solid-State Laser Engineering, Springer Series in Optical Sciences, Vol.1, p. 748, *Springer-Verlag GmbH,* 978-0-387-29094-2, Berlin, Heidelberg

Koopmann, P.; Peters, R.; Petermann, K. & Huber, G. (2009a). Highly Efficient, Broadly Tunable Tm:Lu_2O_3 Laser at 2 μm, *CLEO EUROPE 2009,* CA10.3

Koopmann, P.; Peters, R.; Petermann, K. & Huber, G. (2009a). Hocheffizienter Laserbetrieb von $Tm^{3+}:Lu_2O_3$ bei einer Wellenlänge von 2 µm, *DPG Frühjahrstagung 2009 in Hamburg,* Q8.4

Kuznetsov, M.; Hakimi, F.; Spraque, R. & Mooradian, A. (1997). High-Power (>0.5 W CW) Diode-Pumped Vertical-External-Cavity Surface-Emitting Semiconductor Lasers with Circular TEM_{00} Beams, *IEEE Photonics Technol. Lett.,* Vol. 9, pp. 1063

Meleshkevich, M.; Platonov, N.; Gapontsev, D.; Drozhzhin, A.; Sergeev, V. & Gapontsev, V. (2007). 415W Single-Mode CW Thulium Fiber Laser in all-fiber format, *CLEOE-IQEC 2007,* Munich

Melngailis, I. (1963). Maser action in InAs diodes, *Appl. Phys. Lett.,* Vol.2, 9

Moskalev, I. S.; Fedorov, V. V.; Mirov, S. B.; Babushkin, A.; Gapontsev, V. P.; Gapontsev, D. V. & Platonov, N. (2006). Efficient Ho:YAG Laser Resonantly Pumped by Tm-Fiber Laser, *Advanced Solid-State Photonics,*(Optical Society of America, 2006), TuB10

Moulton, P. F.; Rines, G. A.; Slobodtchikov, E. V. Wall, K. F.; Frith, G.; Samson, B: & Carter, A. L. G. (2009). Tm-Doped Fiber Lasers: Fundamentals and Power Scaling, *IEEE J. of Selected Top. in Quant. Electr.,* Vol. 15, No. 1, pp 85-92

Mu, X.; Meissner, H. E. & Lee, H. C. (2009). Thulium Fiber Laser 4-Pass End-Pumped High Efficiency 2.09-µm Ho:YAG Laser, *OSA/CLEO/IQEC 2009*

Nabors, C. D.; Ochoa, J.; Fan, T. Y.; Sanchez, A.; Choi, H. K. & Turner, G. W. (1995). Ho:YAG Laser Pumped By 1.9 µm Diode Lasers, *IEEE J. Quantum Elect,* Vol. 31, 9

Orii, K.; Nakahara, A.; Ozaki, A.; Sakita, T. & Iwasaki, Y. (1981). Choledocholithomy by YAG laser with a choledochofiberscope: case reports of two patients, *Surgery,* 90

Payne, S. A.; Chase, L. L.; Smith, L. K., Kway, W. L. & Krupke, W. F. (1992). Infrared Cross-Section Measurements for Crystals Doped with Er3+, Tm3+, and Ho3+, *IEEE J. of Quant. Electr.,* Vol. 28, No. 11, pp. 2619-2630

Peterson, P.; Gavrielides, A. & Sharma, M. P. (1995). Diode-pumped Tm:YAG solid-state lasers with indirect and direct manifold pumping, *Appl. Phys. B,* 61, 195

Platt, U. & Stutz, J (2008). Differential Optical Absorption Spectroscopy, *Springer-Verlag GmbH,* 978-3-540-21193-8, Berlin, Heidelberg

Rattunde, M.; Mermelstein, C.; Simanowski, S.; Schmitz, J.; Kiefer, R.; Herres, N.; Fuchs, F.; Walther, M. & Wagner, J. (2000). Temperature dependence of thershold current for 1.8 to 2.3 mm (AlGaIn)(AsSb)-based QW diode lasers, *IEEE 27th International Symposium on Compound Semiconductors (ISCS'00),* Monterey, 437

Rattunde, M.; Mermelstein, C.; Schmitz, J.; Kiefer, R.; Pletschen, W.; Walther, M. & Wagner, J. (2002). Comprehensive modeling of the electro-optical-thermal behaviour of (AlGaIn)(AsSb)-based 2.0 µm diode lasers, *Appl. Phys. Lett.,* Vol. 80, 22

Rattunde, M.; Schmitz, J.; Mermelstein, C.; Kiefer, R. & Wagner, J. (2006a). III-Sb-based Type-I QW Diode Lasers, In: *Mid-infrared Semiconductor Optoelectronics* , Krier, A., pp. 131-157, Springer Series in Optical Sciences, ISBN 1-84628-208-X, London

Rattunde, M.; Schmitz, J.; Kaufel,G.; Kelemen, M. T.; Weber, J. & Wagner, J. (2006b). GaSb-based 2.X mm quantum-well diode lasers with low beam divergence and high output power, Appl. Phys. Lett., Vol. 88

Remski, R. L. & Smith, D. J. (1970). Temperature dependence of pulsed Laser Threshold in YAG-ER3+,TM3+,HO3+, *IEEE J. Quantum Electro.,* 6, 11

Rothacher, Th.; Lüthy, W. & Weber, H. P. (1998). Spectral properties of a Tm:Ho:YAG laser in active mirror configuration, *Appl. Phys. B,* 66, pp. 543–546

Schellhorn, M.; Hirt, A. & Kieleck, C. (2003). Ho:YAG laser intracavity pumped by a diode-pumped Tm:YLF, *Opt. Lett,* Vol. 28, 20

Schellhorn, M. (2006). Performance of a Ho:YAG thin-disc laser pumped by a diode-pumped 1.9 µm thulium laser, *Appl. Phys. B*, 85, 4

Schellhorn, M. (2008). High power diode-pumped Tm:YLF laser, *Appl. Phys. B,* Vol. 91, p. 71

Schellhorn, M.; Ngcobo, S. & Bollig, C. (2009). High-power diode – pumped Tm:YLF slab laser, *Appl. Phys. B,* Vol. 94, pp. 195-198

Scholle, K.; Heumann, E. & Huber, G. (2004). Single mode Tm and Tm,Ho:LuAG lasers for LIDAR applications, *Laser Phys. Lett.,* Vol. 1, No. 6, pp. 1-5

Scholle, K. & Fuhrberg, P. (2008). In-band pumping of high-power Ho:YAG lasers by laser diodes at 1.9 µm, *OSA/CLEO/IQEC 2008*

Scholle, K.; Lamrini, S.; Fuhrberg, P.; Rattunde, M. & Wagner, J. (2009). Wavelength stabilization and mode selection of a GaSb-based semiconductor disk laser at 2000 nm by using a Volume Bragg Grating, *CLEO EUROPE 2009,* CB7.4M

Schulz, N.; Hopkins, J.-M.; Rattunde, M.; Burns, D. & Wagner, J. (2008). High-Brightness long-wavelength semiconductor disk lasers, *Laser & Photonics Rev.,* Vol. 2, No. 3

Shen, D. Y.; Abdolvand, A.; Cooper, L. J. & Clarkson, W. A. (2004). Efficient Ho:YAG laser pumped by a cladding-pumped tunable Tm:silica-fibre laser, *Appl. Phys. B,* 79

So, S.; Mackenzie, J. I.; Shepherd, D. P. & Clarkson, W. A.; Betterton, J. G. & Gorton, E. K. (2006a). A power-scaling strategy for longitudinally diode-pumped Tm:YLF lasers, *Appl. Phys. B,* Vol. 84, pp. 389-393

So, S.; Mackenzie, J. I.; Shepherd, D. P. & Clarkson, W. A. (2006b). Intra-cavity side-pumped Ho:YAG laser, *Optics Express,* Vol. 14, No. 22

Sorokina, I. T. & Vodopyanov, K. L. (2003). Solid-State Mid-Infrared Laser Sources, *Springer-Verlag GmbH,* 3-540-00621-4, Berlin-Heidelberg

Stoneman, R. C. & Esterowitz, L. (1992). Intracavity-pumped 2.09-µm Ho:YAG laser, *Opt. Lett.,* Vol. 17, 10

Strom, M. E. (1988). Laser characteristics of a q-switched Ho:Tm:Cr:YAG, *Appl. Opt.,* 27, (20)

Svelto, O. (1998). Principles of Lasers Fourth Edition, *Springer-Verlag GmbH,* 978-0306457487, Berlin, Heidelberg

Teichman, J. M. H.; Schwesinger, W. H., Lackner, J. & Cossman, R. M. (2001). Holmium: YAG laser lithotripsy for gallstones, *Surg. Endosc.,* Vol. 15, pp. 1034-1037

Turri, G.; Sudesh, V.; Richardson, M.; Bass, M.; Toncelli, A. & Tonelli, M. (2008). Temperature-dependent spectroscopic properties of Tm3+ in germinate, silica, and phosphate glasses: A comparative study, *J. of Appl. Phys.,* Vol. 103

Vodopyanov, K. (2003). Pulsed MID-IR Optical Parametric Oscillators, Solid-State Mid-Infrared Laser Sources, Sorokina, I. T. & Vodopyanov, K. L. *Springer-Verlag GmbH,* 3-540-00621-4, Berlin-Heidelberg

Walsh, B. M.; Barnes, N. P. & Di Bartolo, B. (1998). Branching ratios, cross sections, and radiative lifetimes of rare earth ions in solids: Application to Tm^{3+} and Ho^{3+} ions in $LiYF_4$, *J. of Appl. Phys.,* Vol. 83, No. 5, pp. 2772-2787

Wu, J.; Yao, Z.; Zong, J. & Jiang, S. (2007). Highly efficient high-power thulium-doped germanate glass fiber laser, *Optics Letters,* Vol. 32, No. 6, pp. 638-640

Frontiers in Guided Wave Optics and Optoelectronics

Edited by Bishnu Pal

As the editor, I feel extremely happy to present to the readers such a rich collection of chapters authored/co-authored by a large number of experts from around the world covering the broad field of guided wave optics and optoelectronics. Most of the chapters are state-of-the-art on respective topics or areas that are emerging. Several authors narrated technological challenges in a lucid manner, which was possible because of individual expertise of the authors in their own subject specialties. I have no doubt that this book will be useful to graduate students, teachers, researchers, and practicing engineers and technologists and that they would love to have it on their book shelves for ready reference at any time.

How to reference

In order to correctly reference this scholarly work, feel free to copy and paste the following:

Karsten Scholle, Samir Lamrini, Philipp Koopmann and Peter Fuhrberg (2010). 2 µm Laser Sources and Their Possible Applications, Frontiers in Guided Wave Optics and Optoelectronics, Bishnu Pal (Ed.), ISBN: 978-953-7619-82-4, InTech, Available from: http://www.intechopen.com/books/frontiers-in-guided-wave-optics-and-optoelectronics/2-m-laser-sources-and-their-possible-applications

INTECH
open science | open minds